

Space Mapping: The State of the Art

John W. Bandler, *Fellow, IEEE*, Qingsha S. Cheng, *Student Member, IEEE*,
Sameh A. Dakroury, *Student Member, IEEE*, Ahmed S. Mohamed, *Student Member, IEEE*,
Mohamed H. Bakr, *Member, IEEE*, Kaj Madsen, and Jacob Søndergaard

Abstract—We review the space-mapping (SM) technique and the SM-based surrogate (modeling) concept and their applications in engineering design optimization. For the first time, we present a mathematical motivation and place SM into the context of classical optimization. The aim of SM is to achieve a satisfactory solution with a minimal number of computationally expensive “fine” model evaluations. SM procedures iteratively update and optimize surrogates based on a fast physically based “coarse” model. Proposed approaches to SM-based optimization include the original algorithm, the Broyden-based aggressive SM algorithm, various trust-region approaches, neural SM, and implicit SM. Parameter extraction is an essential SM subproblem. It is used to align the surrogate (enhanced coarse model) with the fine model. Different approaches to enhance uniqueness are suggested, including the recent gradient parameter-extraction approach. Novel physical illustrations are presented, including the cheese-cutting and wedge-cutting problems. Significant practical applications are reviewed.

Index Terms—Computer-aided design (CAD), design automation, electromagnetic (EM) simulation, EM optimization, filter design, microwave filters, optimization algorithms, optimization methods, parameter extraction (PE), space mapping (SM), surrogate models.

I. INTRODUCTION

ENGINEERS have been using optimization techniques for device, component, and system modeling and computer-aided design (CAD) for decades [1]. The target of component design is to determine a set of physical parameters to satisfy certain design specifications. Traditional optimization techniques [2], [3] directly utilize the simulated responses and possibly available derivatives to force the responses to satisfy the design specifications. Circuit-theory-based simulation and CAD tools using empirical device models are fast: analytical solutions or available exact derivatives may promote optimization convergence. Electromagnetic (EM) simulators, long used for design verification, need to be exploited in the optimization process. However, the higher the fidelity (accuracy) of the simulation,

Manuscript received December 3, 2002; revised June 2, 2003. This work was supported in part by the Natural Sciences and Engineering Research Council of Canada under Grant OGP0007239 and Grant STR234854-00, by the Micronet Network of Centres of Excellence, and by Bandler Corporation.

J. W. Bandler is with the Simulation Optimization Systems Research Laboratory, Department of Electrical and Computer Engineering, McMaster University, Hamilton, ON, Canada L8S 4K1 and also with Bandler Corporation, Dundas, ON, Canada L9H 5E7 (e-mail: bandler@mcmaster.ca).

Q. S. Cheng, S. A. Dakroury, and A. S. Mohamed are with the Simulation Optimization Systems Research Laboratory, Department of Electrical and Computer Engineering, McMaster University, Hamilton, ON, Canada L8S 4K1.

M. H. Bakr is with the Department of Electrical and Computer Engineering, McMaster University, Hamilton, ON, Canada L8S 4K1.

K. Madsen and J. Søndergaard are with Informatics and Mathematical Modelling, Technical University of Denmark, DK-2800, Lyngby, Denmark.

Digital Object Identifier 10.1109/TMTT.2003.820904

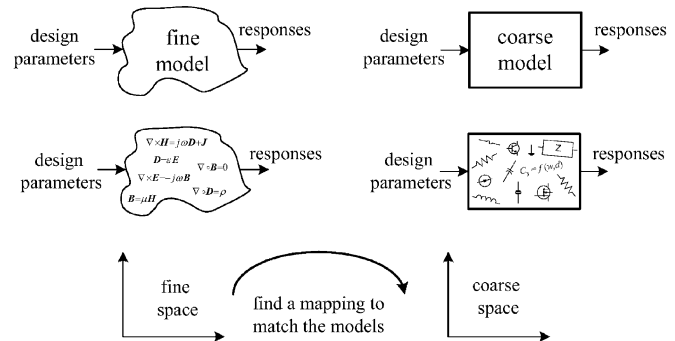


Fig. 1. Linking companion coarse (empirical) and fine (EM) models through a mapping.

the more expensive direct optimization is expected to be. For complex problems, this cost may be prohibitive.

Alternative design schemes combining the speed and maturity of circuit simulators with the accuracy of EM solvers are desirable. The recent exploitation of iteratively refined surrogates of fine, accurate, or high-fidelity models, and the implementation of space mapping (SM) methodologies address this issue. Through the construction of an SM, a suitable surrogate is obtained. This surrogate is faster than the “fine” model and at least as accurate as the underlying “coarse” model. The SM approach updates the surrogate to better approximate the corresponding fine model.

This paper reviews the state of the art of the SM approach, conceived by Bandler in 1993, for modeling and design of engineering devices and systems, e.g., RF and microwave components using EM simulators. Bandler *et al.* [4], [5] demonstrated how SM intelligently links companion “coarse” (ideal, fast, or low fidelity) and “fine” (accurate, practical, or high fidelity) models of different complexities. An EM simulator could serve as a fine model. A low-fidelity EM simulation or empirical circuit model could be a coarse model (see Fig. 1). More model classifications are listed in Table I.

Generally, SM-based optimization algorithms comprise four steps. They are as follows.

- Step 1) Fine model simulation (verification).
- Step 2) Extraction of the parameters of a coarse or surrogate model.
- Step 3) Updating the surrogate.
- Step 4) (Re)optimization of the surrogate.

The original SM-based optimization algorithm was introduced in 1994 [4], where a linear mapping is assumed between the parameter spaces of the coarse and fine models. It is evaluated by a least squares solution of the linear equations

TABLE I
CLASSIFICATION OF MODELS

Model	Classification
Companion	coarse
Low Fidelity	coarse
High Fidelity	fine
Empirical	coarse
Physics-based	coarse or fine
Device under Test	fine
Electromagnetic	fine or coarse
Simulation	fine or coarse
Computational	fine or coarse
Mapped Coarse Model	surrogate

resulting from associating corresponding data points in the two spaces. Hence, the surrogate is a linearly mapped coarse model.

The aggressive space mapping (ASM) approach [5] eliminates the simulation overhead required in [4] by exploiting each fine model iterate as soon as it is available. This iterate, determined by a quasi-Newton step, optimizes the (current) surrogate model.

Parameter extraction (PE) is the key to establishing the mapping and updating the surrogate. In this step, the surrogate is locally aligned with a given fine model through various techniques. However, nonuniqueness of the PE step may cause breakdown of the algorithm [6].

Many approaches are suggested to improve the uniqueness of the PE step. Multipoint parameter extraction (MPE) [6], [7], a statistical PE [7], a penalty PE [8], and an aggressive PE [9] are such approaches. A recent gradient parameter extraction (GPE) approach [10] takes into account not only the responses of the fine model and the surrogate, but the corresponding gradients with respect to design parameters as well.

In this paper, we present for the first time a mathematical motivation and place SM into the context of classical optimization based on local Taylor approximations. If the nonlinearity of the fine model is reflected by the coarse model, then the SM is expected to involve less curvature (less nonlinearity) than the two physical models. The SM model is then expected to yield a good approximation over a large region, i.e., it generates large descent iteration steps. Close to the solution, however, only small steps are needed, in which case, the classical optimization strategy based on local Taylor models is better. A combination of the two strategies gives the highest solution accuracy and fast convergence.

Trust-region strategies were introduced into optimization algorithms to stabilize the iterative process [11]. The trust-region ASM algorithm [12] integrates such a methodology with the SM technique.

SM techniques require sufficiently faithful coarse models to assure good results. Sometimes the coarse model and fine models are severely misaligned, i.e., it is hard to make the PE process work. The hybrid ASM algorithm [13] overcomes this by alternating between (re)optimization of a surrogate and direct response matching. More recently, the surrogate-model-based SM [14] optimization algorithm combines a mapped coarse model with a linearized fine model and defaults to direct optimization of the fine model.

Neural space-mapping (NSM) approaches [15]–[17] utilize artificial neural networks (ANNs) in EM-based modeling and design of microwave devices. This is consistent with the knowledge-based modeling techniques of Zhang and Gupta [18]. After updating an ANN-based surrogate [15], a fine model optimal design is predicted in NSM [16] by (re)optimizing the surrogate. Neural inverse space mapping (NISM) simplifies (re)optimization by inversely connecting the ANN [17]. The next fine model iterate is then only an ANN evaluation.

The latest development of SM is implicit space mapping (ISM) [19]. An auxiliary set of parameters (selected preassigned parameters such as dielectric constant or substrate height) is extracted to match the coarse and fine model responses. The resulting (calibrated) coarse model, the surrogate, is then (re)optimized to evaluate the next iterate (fine model point).

The SMX [20] system is a first attempt to automate SM optimization through linking different simulators.

Several SM-based model enhancement approaches have been proposed: the generalized space-mapping (GSM) tableau approach [21], space derivative mapping [22], and SM-based neuromodeling [15].

The SM technology has been recognized as a contribution to engineering design [18], [23]–[27], especially in the microwave and RF arena. Zhang and Gupta [18] have considered the integration of the SM concept into neural-network modeling for RF and microwave design. Hong and Lancaster [23] describe the ASM algorithm as an elegant approach to microstrip filter design. Conn *et al.* [24] have stated that trust-region methods have been effective in the SM framework, especially in circuit design. Bakr [25] introduces advances in SM algorithms, Rayas-Sánchez [26] employs ANNs, and Ismail [27] studies SM-based model enhancement.

Mathematicians are addressing mathematical interpretations of the formulation and convergence issues of SM algorithms [28]–[35]. For example, Madsen's group [28]–[31] considers the SM as an effective preprocessor for engineering optimizations. Madsen and Søndergaard investigate convergence properties of SM algorithms [32]. Vicente studies convergence properties of SM for design using the least squares formulation [33], [34] and introduces SM to solve optimal control problems [35].

Section II presents a formulation of the SM concept. Section III addresses the original SM optimization algorithm. The ASM algorithm is described in Section IV. PE and different approaches for ensuring uniqueness are reviewed in Section V. In Section VI, a mathematical motivation is presented: SM is placed into the context of classical optimization. Trust-region algorithms are discussed in Section VII, the hybrid- and surrogate-model-based optimization algorithms in Section VIII, the ISM approach in Section IX, device model enhancement (quasi-global modeling) in Section X, neural approaches in Section XI,

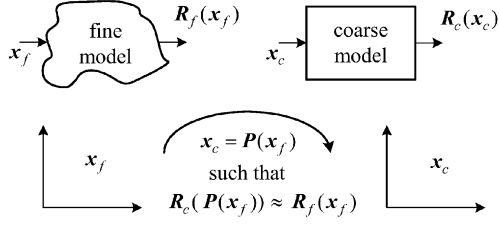


Fig. 2. Illustration of the fundamental notation of SM [1].

and a review of various applications and implementations in Section XII. The discussion and a glossary of terms in Section XIII are followed by conclusions in Section XIV.

II. SM CONCEPT

The SM approach introduced by Bandler *et al.* [4] involves a calibration of a physically based “coarse” surrogate by a “fine” model to accelerate design optimization. This simple CAD methodology embodies the learning process of a designer. It makes effective use of the surrogate’s fast evaluation to sparingly manipulate the iterations of the fine model.

A. Optimization Problem

The design optimization problem to be solved is given by

$$\mathbf{x}^* \triangleq \arg \min_{\mathbf{x}} U(\mathbf{R}(\mathbf{x})) \quad (1)$$

where $\mathbf{R} \in \mathfrak{R}^{m \times 1}$ is a vector of m responses of the model, e.g., $|S_{11}|$ at m selected frequency points, \mathbf{x} is the vector of n design parameters, and U is a suitable objective function. For example, U could be the minimax objective function with upper and lower specifications. \mathbf{x}^* is the optimal solution to be determined. It is assumed to be unique.

B. SM Concept

As depicted in Fig. 2, the coarse and fine model design parameters are denoted by \mathbf{x}_c and $\mathbf{x}_f \in \mathfrak{R}^{n \times 1}$, respectively. The corresponding response vectors are denoted by \mathbf{R}_c and $\mathbf{R}_f \in \mathfrak{R}^{m \times 1}$, respectively.

We propose to find a mapping \mathbf{P} relating the fine and coarse model parameters as

$$\mathbf{x}_c = \mathbf{P}(\mathbf{x}_f) \quad (2)$$

such that

$$\mathbf{R}_c(\mathbf{P}(\mathbf{x}_f)) \approx \mathbf{R}_f(\mathbf{x}_f) \quad (3)$$

in a region of interest.

We can then avoid using direct optimization, i.e., solving (1) to find \mathbf{x}_f^* . Instead, we declare $\bar{\mathbf{x}}_f$, given by

$$\bar{\mathbf{x}}_f \triangleq \mathbf{P}^{-1}(\mathbf{x}_c^*) \quad (4)$$

as a good estimate of \mathbf{x}_f^* , where \mathbf{x}_c^* is the result of coarse model optimization.

C. Jacobian Relationships

Using (2), the Jacobian of \mathbf{P} is given by

$$\mathbf{J}_P \triangleq \mathbf{J}_P(\mathbf{x}_f) = \left(\frac{\partial \mathbf{P}^T}{\partial \mathbf{x}_f} \right)^T = \left(\frac{\partial (\mathbf{x}_c^T)}{\partial \mathbf{x}_f} \right)^T. \quad (5)$$

An approximation to the mapping Jacobian is designated by the matrix $\mathbf{B} \in \mathfrak{R}^{n \times n}$, i.e., $\mathbf{B} \approx \mathbf{J}_P(\mathbf{x}_f)$. Using (3), we obtain [13]

$$\mathbf{J}_f \approx \mathbf{J}_c \mathbf{B} \quad (6)$$

where \mathbf{J}_f and \mathbf{J}_c are the Jacobians of the fine and coarse models, respectively. This relation can be used to estimate the fine model Jacobian if the mapping is already established.

An expression for \mathbf{B} , which satisfies (6), can be derived as [13]

$$\mathbf{B} = (\mathbf{J}_c^T \mathbf{J}_c)^{-1} \mathbf{J}_c^T \mathbf{J}_f. \quad (7)$$

If the coarse and fine model Jacobians are available, the mapping can be established through (7) provided that \mathbf{J}_c has full rank and $m \geq n$.

D. Interpretation of SM Optimization

SM algorithms initially optimize the coarse model to obtain the optimal design \mathbf{x}_c^* , for instance, in the minimax sense. Subsequently, a mapped solution is found by minimizing the objective function $\|\mathbf{g}\|_2^2$, where \mathbf{g} is defined by

$$\mathbf{g} = \mathbf{g}(\mathbf{x}_f) \triangleq \mathbf{R}_f(\mathbf{x}_f) - \mathbf{R}_c(\mathbf{x}_c^*). \quad (8)$$

Correspondingly, according to [28], $\mathbf{R}_c(\mathbf{P}(\mathbf{x}_f))$ is optimized in the effort of finding a solution to (1). Here, $\mathbf{R}_c(\mathbf{P}(\mathbf{x}_f))$ is an expression of an “enhanced” coarse model or “surrogate.” Thus, the problem formulation can be rewritten as

$$\bar{\mathbf{x}}_f = \arg \min_{\mathbf{x}_f} U(\mathbf{R}_c(\mathbf{P}(\mathbf{x}_f))) \quad (9)$$

where $\bar{\mathbf{x}}_f$ may be close to \mathbf{x}_f^* if \mathbf{R}_c is close enough to \mathbf{R}_f . If \mathbf{x}_c^* is unique, then the solution of (9) is equivalent to driving the following residual vector \mathbf{f} to zero:

$$\mathbf{f} = \mathbf{f}(\mathbf{x}_f) \triangleq \mathbf{P}(\mathbf{x}_f) - \mathbf{x}_c^*. \quad (10)$$

III. ORIGINAL SM APPROACH [4]

In this approach, an initial approximation of the mapping $\mathbf{P}^{(0)}$ is obtained by performing fine model analyses at a pre-selected set of at least m_0 base points $m_0 \geq n + 1$. One base point may be taken as the optimal coarse model solution, thus, $\mathbf{x}_f^{(1)} = \mathbf{x}_c^*$. The remaining $m_0 - 1$ base points are chosen by perturbation. A corresponding set of coarse model points is then constructed through the PE process

$$\mathbf{x}_c^{(j)} \triangleq \arg \min_{\mathbf{x}_c} \left\| \mathbf{R}_f(\mathbf{x}_f^{(j)}) - \mathbf{R}_c(\mathbf{x}_c) \right\| \quad (11)$$

for which

$$\varepsilon \triangleq \left\| \mathbf{R}_f(\mathbf{x}_f^{(j)}) - \mathbf{R}_c(\mathbf{x}_c^{(j)}) \right\| = \min_{\mathbf{x}_c} \left\| \mathbf{R}_f(\mathbf{x}_f^{(j)}) - \mathbf{R}_c(\mathbf{x}_c) \right\| \quad (12)$$

is the PE error.

The additional $m_0 - 1$ points apart from $\mathbf{x}_f^{(1)}$ are required to establish full-rank conditions leading to the first mapping approximation $\mathbf{P}^{(0)}$. Bandler *et al.* [4] assumed a linear mapping between the two spaces, i.e.,

$$\mathbf{x}_c = \mathbf{P}^{(j)}(\mathbf{x}_f) = \mathbf{B}^{(j)}\mathbf{x}_f + \mathbf{c}^{(j)} \quad (13)$$

where $\mathbf{B}^{(j)} \in \mathfrak{R}^{n \times n}$ and $\mathbf{c}^{(j)} \in \mathfrak{R}^{n \times 1}$.

At the j th iteration, the sets of points in the two spaces may be expanded to contain, in general, m_j points, which are used to establish the updated mapping $\mathbf{P}^{(j)}$. Since the analytical form of \mathbf{P} is not available, SM uses the current approximation $\mathbf{P}^{(j)}$ to estimate \mathbf{x}_f^* at the j th iteration as

$$\bar{\mathbf{x}}_f \approx \mathbf{x}_f^{(m_j+1)} = \left(\mathbf{P}^{(j)}\right)^{-1}(\mathbf{x}_c^*). \quad (14)$$

The process continues iteratively until $\mathbf{R}_f(\mathbf{x}_f^{(m_j+1)})$ is close enough to $\mathbf{R}_c(\mathbf{x}_c^*)$. If so, $\mathbf{P}^{(j)}$ is assumed close enough to our desired \mathbf{P} . If not, the set of base points in the fine space is augmented by $\mathbf{x}_f^{(m_j+1)}$, and $\mathbf{x}_c^{(m_j+1)}$, as determined by (11), augments the set of base points in the coarse space. Upon termination, we set the space-mapped design as in (14).

This algorithm is simple, but has pitfalls. First, m_0 up-front high-cost fine model analyses are needed. Second, a linear mapping may not be valid for significantly misaligned models. Third, nonuniqueness in the PE process may lead to an erroneous mapping estimation and algorithm breakdown.

IV. ASM APPROACH [5]

The ASM algorithm incorporates a quasi-Newton iteration using the classical Broyden formula [36]. A rapidly improved design is anticipated following each fine model simulation, while the bulk of the computational effort (optimization, PE) is carried out in the coarse model space.

A. Theory

The ASM technique iteratively solves the nonlinear system

$$\mathbf{f}(\mathbf{x}_f) = \mathbf{0} \quad (15)$$

for \mathbf{x}_f . Note, from (10), that at the j th iteration, the error vector $\mathbf{f}^{(j)}$ requires an evaluation of $\mathbf{P}^{(j)}(\mathbf{x}_f^{(j)})$. This is executed indirectly through the PE (evaluation of $\mathbf{x}_c^{(j)}$). Coarse model optimization produces \mathbf{x}_c^*

The quasi-Newton step in the fine space is given by

$$\mathbf{B}^{(j)}\mathbf{h}^{(j)} = -\mathbf{f}^{(j)} \quad (16)$$

where $\mathbf{B}^{(j)}$, the approximation of the mapping Jacobian \mathbf{J}_P , defined in (5), is updated using Broyden's rank one update. Solving (16) for $\mathbf{h}^{(j)}$ provides the next iterate $\mathbf{x}_f^{(j+1)}$

$$\mathbf{x}_f^{(j+1)} = \mathbf{x}_f^{(j)} + \mathbf{h}^{(j)}. \quad (17)$$

The algorithm terminates if $\|\mathbf{f}^{(j)}\|$ becomes sufficiently small. The output of the algorithm is an approximation to

$\bar{\mathbf{x}}_f = \mathbf{P}^{-1}(\mathbf{x}_c^*)$ and the mapping matrix \mathbf{B} . The matrix \mathbf{B} can be obtained in several ways.

B. Unit Mapping

A "steepest descent" approach may succeed if the mapping between the two spaces is essentially represented by a shift. In this case, Broyden's updating formula is not utilized. We can solve (16) keeping the matrix $\mathbf{B}^{(j)}$ fixed at $\mathbf{B}^{(j)} = \mathbf{I}$. Bila *et al.* [37] and Pavio [38] utilized this special case.

C. Broyden-Like Updates

An initial approximation to \mathbf{B} can be taken as $\mathbf{B}^{(0)} = \mathbf{I}$, the identity matrix. $\mathbf{B}^{(j)}$ can be updated using Broyden's rank one formula [36]

$$\mathbf{B}^{(j+1)} = \mathbf{B}^{(j)} + \frac{\mathbf{f}^{(j+1)} - \mathbf{f}^{(j)} - \mathbf{B}^{(j)}\mathbf{h}^{(j)}}{\mathbf{h}^{(j)T}\mathbf{h}^{(j)}}\mathbf{h}^{(j)T}. \quad (18)$$

When $\mathbf{h}^{(j)}$ is the quasi-Newton step, (18) can be simplified using (16) to

$$\mathbf{B}^{(j+1)} = \mathbf{B}^{(j)} + \frac{\mathbf{f}^{(j+1)}}{\mathbf{h}^{(j)T}\mathbf{h}^{(j)}}\mathbf{h}^{(j)T}. \quad (19)$$

D. Jacobian-Based Updates

If we have exact Jacobians with respect to \mathbf{x}_f and \mathbf{x}_c at corresponding points, we can use them to obtain \mathbf{B} at each iteration through a least squares solution [10], [13], as given in (7).

Note that \mathbf{B} can be fed back into the PE process and iteratively refined before making a step in the fine model space.

Hybrid schemes can be developed following the integrated gradient approximation approach to optimization [39]. One approach incorporates finite-difference approximations and the Broyden formula [10]. Finite-difference approximations could provide initial estimates of \mathbf{J}_f and \mathbf{J}_c . These are then used to obtain a good approximation to $\mathbf{B}^{(0)}$. The Broyden formula is subsequently used to update \mathbf{B} .

E. Constrained Update [40]

On the assumption that the fine and coarse models share the same physical background, Bakr *et al.* [40] suggested that \mathbf{B} could be better conditioned in the PE process if it is constrained to be close to the identity matrix \mathbf{I} by letting

$$\mathbf{B} = \arg \min_{\mathbf{B}} \left\| \left[\mathbf{e}_1^T \cdots \mathbf{e}_n^T \quad \eta \Delta \mathbf{b}_1^T \cdots \eta \Delta \mathbf{b}_n^T \right]^T \right\|_2^2. \quad (20)$$

where η is a user-assigned weighting factor, \mathbf{e}_i and $\Delta \mathbf{b}_i$ are the i th columns of \mathbf{E} and $\Delta \mathbf{B}$, respectively, defined as

$$\begin{aligned} \mathbf{E} &= \mathbf{J}_f - \mathbf{J}_c \mathbf{B} \\ \Delta \mathbf{B} &= \mathbf{B} - \mathbf{I}. \end{aligned} \quad (21)$$

The analytical solution of (20) is given by

$$\mathbf{B} = \left(\mathbf{J}_c^T \mathbf{J}_c + \eta^2 \mathbf{I} \right)^{-1} \left(\mathbf{J}_c^T \mathbf{J}_f + \eta^2 \mathbf{I} \right). \quad (22)$$

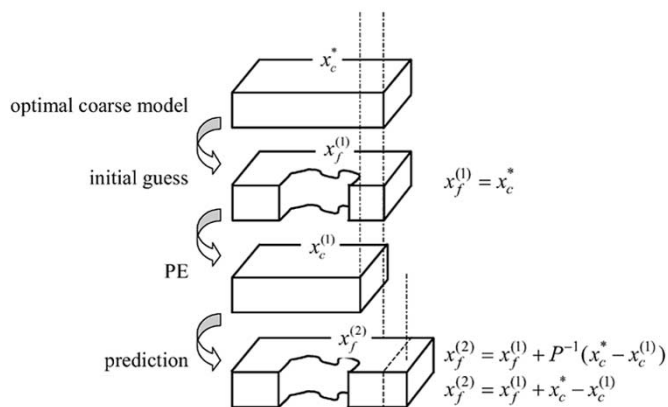


Fig. 3. Cheese-cutting problem solved by ASM of model lengths.

F. Cheese-Cutting Problem

This simple physical example, depicted in Fig. 3, demonstrates the ASM approach. Our “response” is *weight*. The designable parameter is *length*. A density of one assumed. The goal is a desired *weight*.

Our idealized “coarse” model is a uniform cuboidal block (top block of Fig. 3). The optimal *length* x_c^* is easily calculated.

Let the actual block (“fine” model) be similar, but imperfect (second block of Fig. 3). We take the optimal coarse model *length* as the initial guess for the fine model solution, i.e., cutting the cheese so that $x_f^{(1)} = x_c^*$. This does not satisfy our goal. We realign our coarse model to match the outcome of the cut. This is a PE step in which we obtain a solution $x_c^{(1)}$ (third block of Fig. 3). Thus, we have corresponding values $x_f^{(1)}$ and $x_c^{(1)}$. Assuming a unit mapping, we can write for $j = 1$

$$x_f^{(j+1)} = x_f^{(j)} + x_c^* - x_c^{(j)} \tag{23}$$

to predict the next fine model *length* (last block of Fig. 3).

Note that we assume that the actual block (fine model) perfectly matches its coarse model, except for the missing piece; also that the first and second attempts (cuts) to achieve our goal are confined to a uniform section. Our goal is achieved in one space-mapping step, a result consistent with expectations.

Observe that the *length* of the coarse model is shrunk during PE to match our first outcome. The difference between the proposed initial *length* of the block and the shrunk *length* is applied through the (unit) mapping to predict a new cut. This procedure can be repeated until the goal is satisfied.

G. Five-Pole Interdigital Filter [8]

Interdigital filters [41], [42] have the advantage of compact size and adaptability to narrow- and wide-band applications. A five-pole interdigital filter is shown in Fig. 4. It consists of five quarter-wavelength resonators, as well as input and output microstrip T-junctions within a shielded box. Each resonator is formed by one quarter-wavelength microstrip-line (MSL) section, shorted by a via at one end and opened at the other end. The arrows in Fig. 4 indicate the input and output reference planes, and the triangles symbolize the grounded vias.

Decomposition is used to construct a coarse model. As shown in Fig. 5, the coarse filter has a 12-port center piece, the vias, the

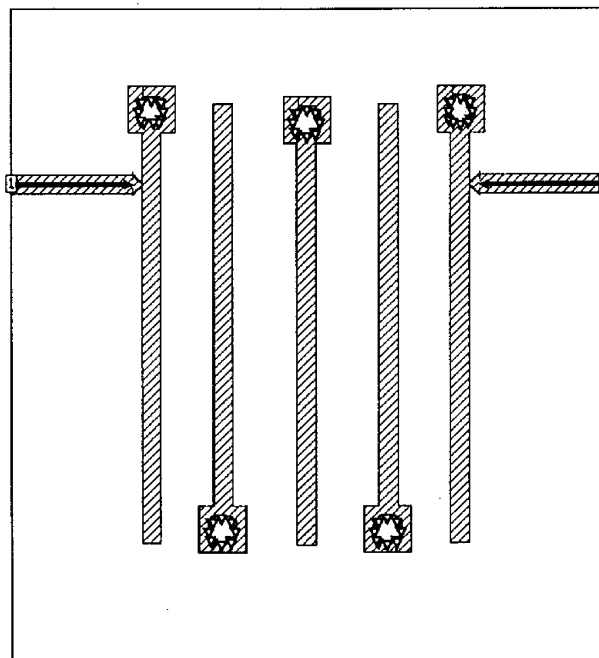


Fig. 4. Five-pole interdigital filter [8].

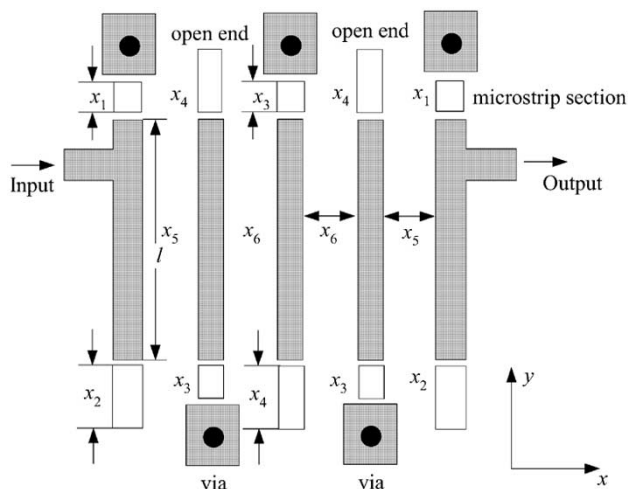


Fig. 5. Coarse model of the five-pole interdigital filter using decomposition [8].

MSL sections, and the open ends. The vias are analyzed by *em*¹ with a fine grid. All the other parts are analyzed using coarse grid *em* or empirical models in OSA90/hope.² The results are then connected through circuit theory to obtain the responses of the overall filter.

The alumina substrate height is 15 mil with $\epsilon_r = 9.8$. The width of each microstrip is chosen as 10 mil. The optimization variables are chosen to be x_1, x_2, \dots, x_6 , as shown in Fig. 5.

The interdigital filter design specifications are as follows:

- Passband ripple ≤ 0.1 dB for $4.9 \text{ GHz} \leq \omega \leq 5.3 \text{ GHz}$
- Isolation: 30 dB, Isolation bandwidth: 0.95 GHz

¹*em* version 5.1a, Sonnet Software, Inc., Liverpool, NY, 1997.
²OSA90/hope, formerly Optimization Systems Associates Inc., Dundas, ON, Canada, 1997.

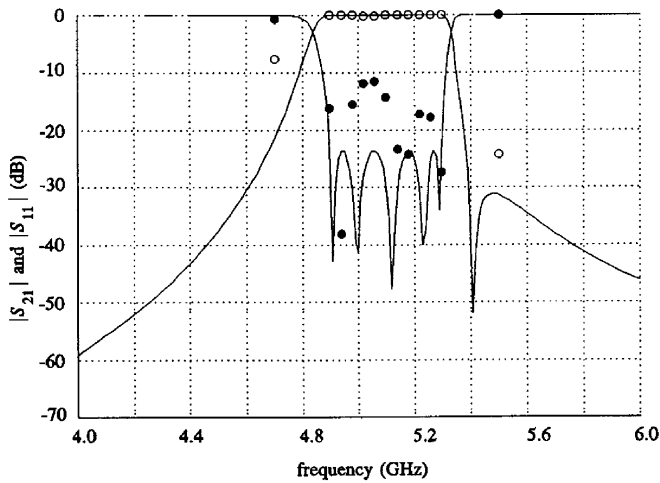


Fig. 6. Optimal coarse model target response ($-|S_{11}|$ and $|S_{21}|$) and the fine model response at the starting point ($\bullet|S_{11}|$ and $\circ|S_{21}|$) for the five-pole interdigital filter [8].

Sonnet's *em* driven by Empipe³ is employed as the fine model, using a high-resolution grid with a 1 mil \times 1 mil cell size. With this grid size, the EM simulation time is approximately 1.5 CPU h per frequency point on a Sun SPARCstation 10. The coarse model simulation takes less than 1.5 CPU min per frequency point on a Sun SPARCstation 10. The overall CPU time required for optimizing the coarse model is approximately 2 h, which is the same order of magnitude as the fine-model EM simulation at a single frequency point.

The ASM technique converges in two iterations. The coarse and fine model responses at the optimal coarse model solution are shown in Fig. 6. The optimal coarse model response and the final fine model response are shown in Fig. 7. The final fine model response using a fine frequency sweep is shown in Fig. 8. The passband return loss is better than 18.5 dB and the insertion loss ripples are less than 0.1 dB.

V. PE

PE is crucial to successful SM. Typically, an optimization process extracts the parameters of a coarse model or surrogate to match the fine model. Inadequate response data in the PE process may lead to nonunique solutions. Sufficient data to overdetermine a solution should be sought. For example, we may use responses such as real and imaginary parts of the S -parameters in the PE even though the design criteria may include the magnitude of S_{11} only.

A. Single-Point Parameter Extraction (SPE) [4]

The traditional SPE is described by the optimization problem given in (11). It is simple and works in many cases.

B. MPE [6], [7]

The MPE approach simultaneously matches the responses at a number of corresponding points in the coarse and fine model spaces. A set $V = \{\mathbf{x}_f^{(j+1)}\} \cup \{\mathbf{x}_f^{(j+1)} + \Delta\mathbf{x}_f^{(i)} | i = 1, 2, \dots, N_p\}$ of fine model points is constructed by selecting

³Empipe, version 4.0, formerly Optimization Systems Associates Inc., Dundas, ON, Canada, 1997.

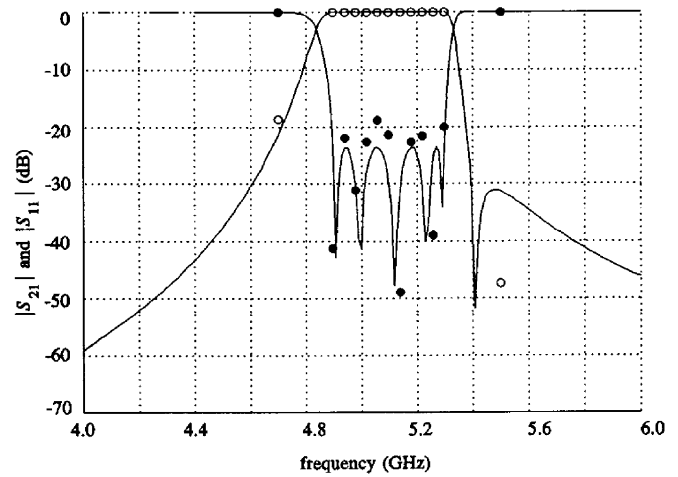


Fig. 7. Optimal coarse model target response ($-|S_{11}|$ and $|S_{21}|$) and the fine model response at the final design ($\bullet|S_{11}|$ and $\circ|S_{21}|$) for the five-pole interdigital filter [8].

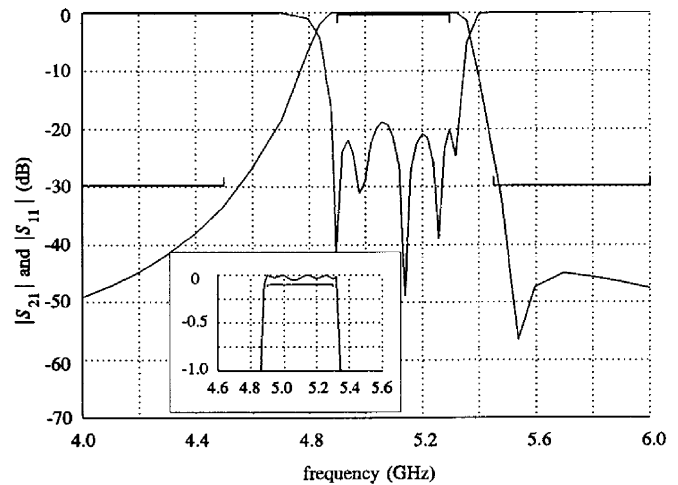


Fig. 8. Fine model response at the final design ($-|S_{11}|$ and $|S_{21}|$) using a fine frequency sweep for the five-pole interdigital filter [8].

N_p perturbations around $\mathbf{x}_f^{(j+1)}$. The corresponding $\mathbf{x}_c^{(j+1)}$ is found by solving

$$\mathbf{x}_c^{(j+1)} = \arg \min_{\mathbf{x}_c} \left\| \begin{bmatrix} \mathbf{e}_0^T & \mathbf{e}_1^T & \dots & \mathbf{e}_{N_p}^T \end{bmatrix}^T \right\| \quad (24)$$

where

$$\mathbf{e}_0 = \mathbf{R}_c(\mathbf{x}_c) - \mathbf{R}_f(\mathbf{x}_f^{(j+1)}) \quad (25)$$

and

$$\mathbf{e}_i = \mathbf{R}_c(\mathbf{x}_c + \Delta\mathbf{x}_c^{(i)}) - \mathbf{R}_f(\mathbf{x}_f^{(j+1)} + \Delta\mathbf{x}_f^{(i)}), \quad i = 1, 2, \dots, N_p. \quad (26)$$

The perturbations $\Delta\mathbf{x}_c^{(i)}$ in (26) are related to $\Delta\mathbf{x}_f^{(i)}$. The basic MPE [6] assumes the relation is given by

$$\Delta\mathbf{x}_c^{(i)} = \Delta\mathbf{x}_f^{(i)}, \quad i = 1, 2, \dots, N_p. \quad (27)$$

This approach to MPE does not provide guidelines on the selection of fine model points.

A more reliable algorithm [12] considers the relation between the perturbations to be determined through the mapping matrix \mathbf{B} . Such a relation is given by

$$\Delta \mathbf{x}_c^{(i)} = \mathbf{B} \Delta \mathbf{x}_f^{(i)}, \quad i = 1, 2, \dots, N_p. \quad (28)$$

The algorithm proposed in [12] also automates the selection of the set of fine model points by recursively augmenting the set V until a unique PE is achieved.

Another improvement in the selection of V is suggested by the aggressive PE algorithm [9], which aims at minimizing the number of points used in MPE. It exploits the gradients and Hessians of the coarse model responses at the extracted point $\mathbf{x}_c^{(j+1)}$ to construct new points to be added to V . A perturbation $\Delta \mathbf{x}_c^{\text{new}}$ is found by solving the eigenvalue problem

$$\left(\mathbf{J}_c(\mathbf{x}_c^{(j+1)})^T \mathbf{J}_c(\mathbf{x}_c^{(j+1)}) + \mathbf{I} \right) \Delta \mathbf{x}_c^{\text{new}} = \lambda \Delta \mathbf{x}_c^{\text{new}}. \quad (29)$$

The corresponding perturbation $\Delta \mathbf{x}_f^{\text{new}}$ is found consistent with (28) and the set V is augmented by

$$\mathbf{x}_f^{\text{new}} = \mathbf{x}_f^{(j+1)} + \Delta \mathbf{x}_f^{\text{new}}. \quad (30)$$

C. Statistical PE [7]

Bandler *et al.* [7] suggest a statistical approach to PE. The SPE process is initiated from several starting points and is declared unique if consistent extracted parameters are obtained. Otherwise, the best solution is selected.

A set of N_s starting points are randomly selected in a region $D \subset \mathfrak{R}^n$ where the solution $\mathbf{x}_c^{(j+1)}$ is expected. For the j th iteration, D is implied by

$$x_{c,i} \in \left[x_{c,i}^* - 2 \left| f_i^{(j)} \right|, x_{c,i}^* + 2 \left| f_i^{(j)} \right| \right], \quad i = 1, 2, \dots, n \quad (31)$$

where $x_{c,i}$ is the i th component of \mathbf{x}_c and f_i is the i th component of \mathbf{f} , as in (10).

D. Penalized PE [8]

Another approach is suggested in [8]. Here, the point $\mathbf{x}_c^{(j+1)}$ is obtained by solving the penalized SPE process

$$\mathbf{x}_c^{(j+1)} = \arg \min_{\mathbf{x}_c} \left\| \mathbf{R}_c(\mathbf{x}_c) - \mathbf{R}_f(\mathbf{x}_f^{(j+1)}) \right\| + w \|\mathbf{x}_c - \mathbf{x}_c^*\| \quad (32)$$

where w is a user-assigned weighting factor. If the PE problem is not unique, (32) is favored over (11), as the solution is biased toward \mathbf{x}_c^* . The process is designed to push the error vector $\mathbf{f} = \mathbf{x}_c - \mathbf{x}_c^*$ to zero. If w is too large, the matching between the responses is poor. On the other hand, too small a value of w makes the penalty term ineffective, in which case, the uniqueness of the extraction step may not be enhanced.

E. PE Involving Frequency Mapping

Alignment of the models might be achieved by simulating the coarse model at a transformed set of frequencies [15]. For example, an EM model of a microwave structure usually exhibits a frequency shift with respect to an idealized representation. Also, available quasi-static empirical models exhibit good accuracy

over a limited range of frequencies, which can be alleviated by frequency transformation.

The PE optimization process (11), which extracts \mathbf{x}_c to correspond to a given \mathbf{x}_f , may fail if the responses \mathbf{R}_f and \mathbf{R}_c are disjoint. However, the responses might be aligned if a frequency transformation $\omega_c = P_\omega(\omega)$ is applied, relating frequency ω to the coarse model frequency ω_c . Frequency mapping introduces new degrees of freedom [14].

A suitable mapping can be as simple as frequency shift and scaling given by [5]

$$\omega_c = P_\omega(\omega) \triangleq \sigma \omega + \delta \quad (33)$$

where σ represents a scaling factor and δ is an offset (shift).

The approach can be divided into two phases [5]. In *Phase 1*, we determine σ_0 and δ_0 that align \mathbf{R}_f and \mathbf{R}_c in the frequency domain. This is done by finding

$$\arg \min_{\sigma_0, \delta_0} \left\| \mathbf{R}_c(\mathbf{x}_c, \sigma_0 \omega_i + \delta_0) - \mathbf{R}_f(\mathbf{x}_f) \right\|, \quad i = 1, 2, \dots, k. \quad (34)$$

In *Phase 2*, the coarse model point \mathbf{x}_c is extracted to match \mathbf{R}_c with \mathbf{R}_f , starting with $\sigma = \sigma_0$ and $\delta = \delta_0$. Three algorithms [5] can implement this phase: a sequential algorithm and two exact-penalty function algorithms, one using the l_1 norm, and the other is suitable for minimax optimization [5].

F. GPE [10]

GPE exploits the availability of exact Jacobians \mathbf{J}_f and \mathbf{J}_c . At the j th iteration, $\mathbf{x}_c^{(j)}$ is obtained through a GPE process. In GPE, we match not only the responses, but also the derivatives of both models through the optimization problem

$$\mathbf{x}_c^{(j)} = \arg \min_{\mathbf{x}_c} \left\| \left[\mathbf{e}_0^T \quad \lambda \mathbf{e}_1^T \quad \dots \quad \lambda \mathbf{e}_n^T \right]^T \right\|, \quad \lambda \geq 0 \quad (35)$$

where λ is a user-assigned weight, $\mathbf{E} = [\mathbf{e}_1 \mathbf{e}_2 \dots \mathbf{e}_n]$, and

$$\begin{aligned} \mathbf{e}_0 &= \mathbf{R}_f(\mathbf{x}_f^{(j)}) - \mathbf{R}_c(\mathbf{x}_c) \\ \mathbf{E} &= \mathbf{J}_f(\mathbf{x}_f^{(j)}) - \mathbf{J}_c(\mathbf{x}_c) \mathbf{B}. \end{aligned} \quad (36)$$

This approach reflects the idea of the MPE [6] process, but permits the use of exact or implementable sensitivity techniques [43]–[48]. Finite differences can be employed to estimate derivatives if exact ones are unavailable.

G. Other Considerations

We can broaden the scope of parameters that are varied in an effort to match the coarse (surrogate) and fine models. We already discussed the scaling factor and shift parameters in the frequency mapping. We can also consider neural weights in NSM, preassigned parameters in ISM, mapping coefficients \mathbf{B} , etc., as in the generalized SM tableau approach [21], and surrogate model-based SM [14].

H. Rosenbrock Example [49]

The Rosenbrock banana function is used to test new optimization algorithms. The minimum is located in a narrow curved valley (Fig. 9). We use this function to illustrate how to resolve the nonuniqueness problem in the crucial PE step.

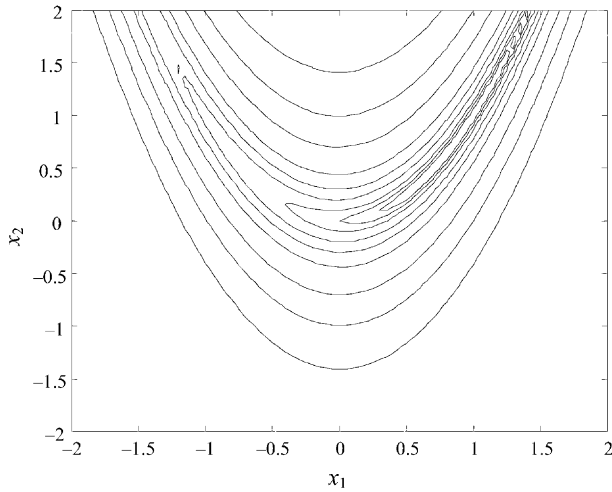


Fig. 9. Contour plot of the "coarse" original Rosenbrock banana function [10].

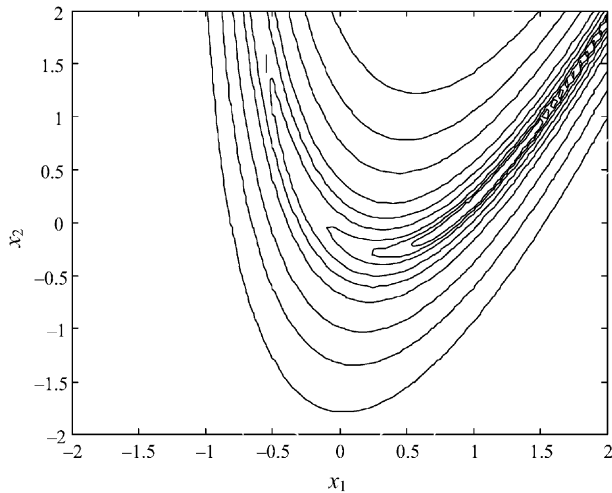


Fig. 10. Contour plot of the "fine" transformed Rosenbrock banana function [10].

The original Rosenbrock function

$$R_c \triangleq 100(x_2 - x_1^2)^2 + (1 - x_1)^2 \quad (37)$$

is taken as a "coarse" model with optimal solution $\mathbf{x}_c^* = [1.0 \ 1.0]^T$. A "fine" model is described by the transformed function

$$R_f \triangleq 100(u_2 - u_1^2)^2 + (1 - u_1)^2 \quad (38)$$

where

$$\mathbf{u} = \begin{bmatrix} 1.1 & -0.2 \\ 0.2 & 0.9 \end{bmatrix} \mathbf{x} + \begin{bmatrix} -0.3 \\ 0.3 \end{bmatrix}. \quad (39)$$

The solution to seven decimals evaluated by the inverse transformation is $\mathbf{x}_f^* = [1.2718447 \ 0.4951456]^T$. Contour plots of the coarse and the fine models are shown in Figs. 9 and 10, respectively.

A simple SPE process involving only function values produces a nonunique solution (Fig. 11). The enhanced PE process such as GPE or MPE leads to improved results. The first and last GPE iterations are shown in Figs. 12 and 13, respectively.

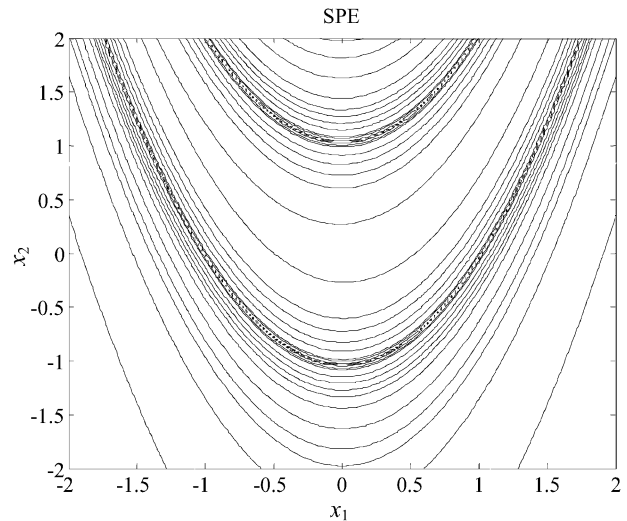


Fig. 11. Nonuniqueness occurs when SPE is used to match the models in the "transformed" Rosenbrock problem.

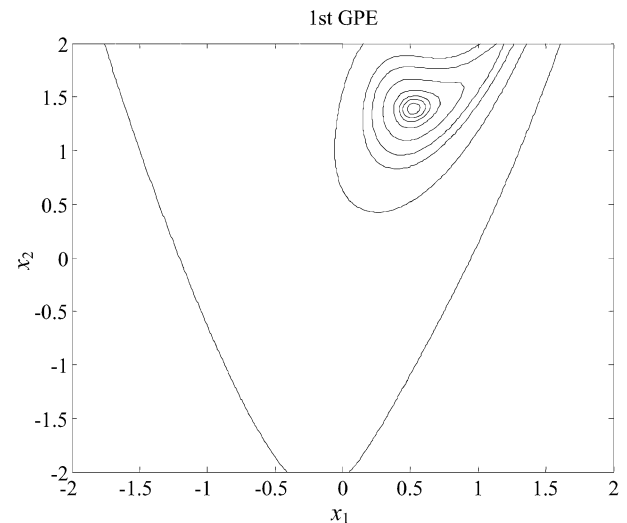


Fig. 12. Unique solution is obtained when GPE is used in the "transformed" Rosenbrock problem in the first iteration.

After six ASM iterations, the algorithm [10] converges to $\mathbf{x}_f = [1.2718 \ 0.4951]^T$. The corresponding function value is 9×10^{-29} . At the final GPE step, the contour plot is similar to that of the coarse model (see Fig. 13). The SM optimization results for \mathbf{R}_f and $\|\mathbf{f}\|$ are shown in Figs. 14 and 15, respectively.

VI. MATHEMATICAL MOTIVATION FOR SM

In this section, we place the SM formulation into the context of classical optimization methods [3], [50]–[54]. These methods are iterative and based on a local Taylor approximation, or rather a local Taylor model, at the current iterate $\mathbf{x}_f^{(j)}$, namely,

$$L_f(\mathbf{x}_f^{(j)} + \mathbf{h}) \triangleq \mathbf{R}_f(\mathbf{x}_f^{(j)}) + \mathbf{J}_f(\mathbf{x}_f^{(j)})\mathbf{h}. \quad (40)$$

The deviation of this model from \mathbf{R}_f can be bounded as

$$\|\mathbf{R}_f(\mathbf{x}_f^{(j)} + \mathbf{h}) - L_f(\mathbf{x}_f^{(j)} + \mathbf{h})\| \leq C_T \|\mathbf{h}\|^2 \quad (41)$$

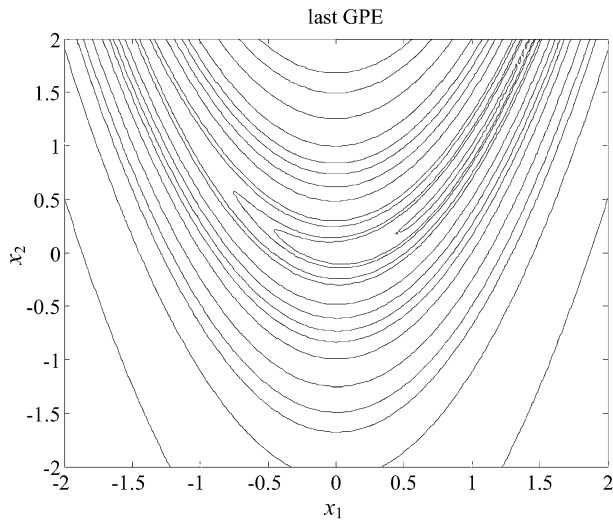
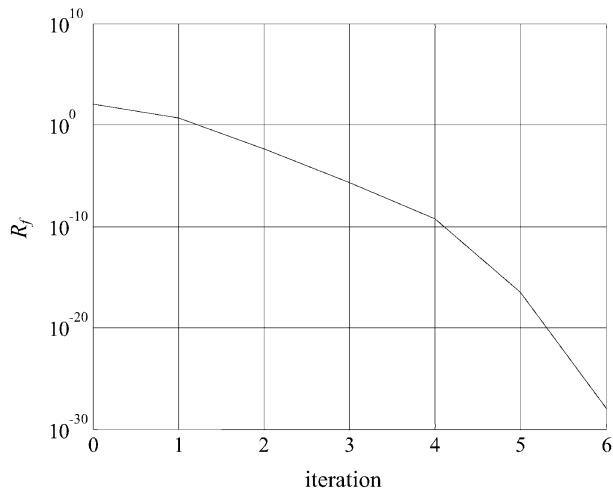
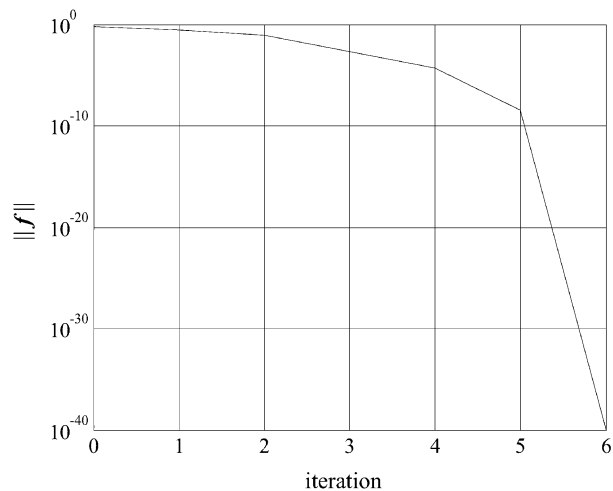


Fig. 13. Sixth (last) GPE iteration of the “transformed” Rosenbrock problem.


 Fig. 14. Reduction of R_f versus iteration count of the “transformed” Rosenbrock problem.

 Fig. 15. Reduction of $\|f\|$ versus iteration count of the “transformed” Rosenbrock problem.

where C_T is a constant. If we make a similar Taylor approximation to \mathbf{P}

$$\mathbf{L}_P(\mathbf{x}_f^{(j)} + \mathbf{h}) \triangleq \mathbf{P}(\mathbf{x}_f^{(j)}) + \mathbf{J}_P(\mathbf{x}_f^{(j)})\mathbf{h} \quad (42)$$

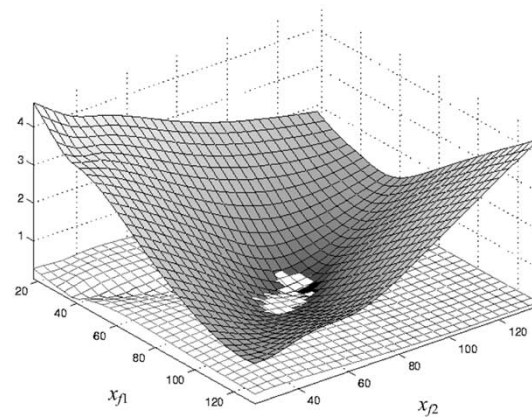


Fig. 16. Model effectiveness plots for a two-section capacitively loaded impedance transformer [28] at the final iterate $\mathbf{x}_f^{(j)}$, approximately $[74.23 \ 79.27]^T$. Centered at $\mathbf{h} = \mathbf{0}$, the light grid shows $\|\mathbf{R}_f(\mathbf{x}_f^{(j)} + \mathbf{h}) - \mathbf{R}_c(\mathbf{L}_P(\mathbf{x}_f^{(j)} + \mathbf{h}))\|$. This represents the deviation of the mapped coarse model (using the Taylor approximation to the mapping, i.e., a linearized mapping) from the fine model. The dark grid shows $\|\mathbf{R}_f(\mathbf{x}_f^{(j)} + \mathbf{h}) - \mathbf{L}_f(\mathbf{x}_f^{(j)} + \mathbf{h})\|$. This is the deviation of the fine model from its classical first-order Taylor approximation. It is seen that the Taylor approximation is most accurate close to $\mathbf{x}_f^{(j)}$, whereas the mapped coarse model is best over a large region.

we have the approximation bound

$$\left\| \mathbf{P}(\mathbf{x}_f^{(j)} + \mathbf{h}) - \mathbf{L}_P(\mathbf{x}_f^{(j)} + \mathbf{h}) \right\| \leq C_P \|\mathbf{h}\|^2 \quad (43)$$

where C_P is a constant. The approximation \mathbf{L}_P to \mathbf{P} is what (13) is designed to realize, where

$$\mathbf{h} = \mathbf{x}_f - \mathbf{x}_f^{(j)}. \quad (44)$$

Assuming this approximation, the difference between \mathbf{R}_f and the mapped coarse model can be bounded as

$$\begin{aligned} \left\| \mathbf{R}_f(\mathbf{x}_f^{(j)} + \mathbf{h}) - \mathbf{R}_c(\mathbf{P}(\mathbf{x}_f^{(j)} + \mathbf{h})) \right\| \\ \leq \varepsilon + C_P \cdot \left\| \mathbf{J}_c(\mathbf{P}(\mathbf{x}_f^{(j)})) \right\| \cdot \|\mathbf{h}\|^2 \end{aligned} \quad (45)$$

where ε is obtained from (12). Thus, unlike the Taylor approximation, the SM does not interpolate at the current iterate $\mathbf{x}_f^{(j)}$ if the PE error $\varepsilon > 0$. This must be considered the normal situation. When \mathbf{x}_f moves away from $\mathbf{x}_f^{(j)}$, the Taylor error increases with the square of $\|\mathbf{h}\|$. As follows from (45), this is also the case for the SM error and, thus, we can only expect the SM model to be better than the Taylor model if C_P is smaller than C_T . This means that \mathbf{P} is “closer to linear” than \mathbf{R}_f , which is a reasonable assumption if the two models \mathbf{R}_c and \mathbf{R}_f are similar: some of the nonlinearity of \mathbf{R}_f then also appears in \mathbf{R}_c . Thus, the mapping \mathbf{P} is simpler, i.e., less nonlinear.

If C_P is considerably smaller than C_T , then the SM model will be more accurate than the Taylor model when $\|\mathbf{h}\|$ is large. However, when \mathbf{x}_f is close to $\mathbf{x}_f^{(j)}$, the Taylor model is always the best provided $\varepsilon > 0$. Fig. 16 contrasts the effectiveness of a mapped coarse model with a classical Taylor model for a two-section capacitively loaded impedance transformer example around the current iterate [28]. It is clear that the SM model is a good approximation over the entire region far from $\mathbf{x}_f^{(j)}$. However, if the solution is very close to $\mathbf{x}_f^{(j)}$, then the classical Taylor model is best.

VII. TRUST REGIONS AND AGGRESSIVE SM

A goal of modern nonlinear programming is robust global behavior of the algorithms. By robust global behavior, we mean the mathematical assurance that the iterates produced by an optimization algorithm, started at an arbitrary initial iterate, will converge to a stationary point or local minimizer for the problem [11]. Trust-region strategies can be used to achieve this property.

A. Trust-Region Methods [24]

The idea of trust-region methods is to adjust the length of the step taken at each iteration based on how well an approximate linear or quadratic model predicts the objective function. The approximate model is trusted to represent the objective function only within a region of specific radius around the current iteration. The local model minimum inside the trust region is found by solving a trust-region subproblem. If the model minimum achieves sufficient actual reduction in the objective function, the trust-region size is increased. If insufficient reduction is achieved, the trust region is reduced. Otherwise the trust region is kept unchanged.

Assume that the objective function is a scalar function $f(\mathbf{x})$. At the j th iterate $\mathbf{x}^{(j)}$, a local approximate model $L^{(j)}(\mathbf{x})$ is used to approximate $f(\mathbf{x})$. It is crucial that $L^{(j)}(\mathbf{x})$ is interpolating f at $\mathbf{x}^{(j)}$, i.e., it has the property

$$L^{(j)}(\mathbf{x}^{(j)} + \mathbf{h}^{(j)}) - f(\mathbf{x}^{(j)}) \rightarrow 0, \quad \text{as } \mathbf{h}^{(j)} \rightarrow 0. \quad (46)$$

The step $\mathbf{h}^{(j)}$ to the next tentative iterate is found by solving the trust-region subproblem

$$\underset{\mathbf{h}}{\text{minimize}} L^{(j)}(\mathbf{x}^{(j)} + \mathbf{h}) \quad (47)$$

subject to

$$\|\mathbf{h}\| \leq \delta^{(j)} \quad (48)$$

where $\delta^{(j)}$ is the trust-region size. A quality measure of the next tentative step $\mathbf{h}^{(j)}$ is the ratio $\rho^{(j)}$ as follows:

$$\rho^{(j)} = \frac{f(\mathbf{x}^{(j)}) - f(\mathbf{x}^{(j)} + \mathbf{h}^{(j)})}{L^{(j)}(\mathbf{x}^{(j)}) - L^{(j)}(\mathbf{x}^{(j)} + \mathbf{h}^{(j)})} \quad (49)$$

where the numerator represents the actual reduction and the denominator is the reduction predicted by the local approximation. The trust-region size is adjusted at the end of each iteration based on $\rho^{(j)}$. The next iteration is accepted only if an actual reduction is achieved in the objective function. A good survey of methods for updating the trust-region size is given in [55].

B. Trust Region and ASM [12]

The trust-region ASM algorithm integrates a trust-region methodology with the ASM technique. Instead of using a quasi-Newton step in the ASM to drive \mathbf{f} to zero, a trust-region subproblem is solved within a certain trust region to minimize $\|\mathbf{f}^{(j+1)}\|_2^2$. Consider the linearized function

$$L^{(j)}(\mathbf{x}^{(j)}, \mathbf{h}^{(j)}) \triangleq \mathbf{f}^{(j)} + \mathbf{B}^{(j)}\mathbf{h}^{(j)}. \quad (50)$$

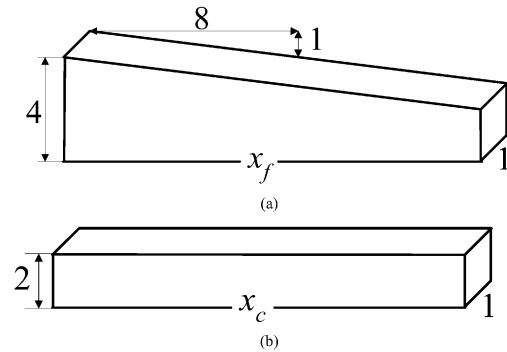


Fig. 17. Wedge problem. (a) Fine model. (b) Possible coarse model.

The next step is obtained by solving the trust-region subproblem

$$\mathbf{h}^{(j)} = \arg \min_{\mathbf{h}} \left\| L^{(j)}(\mathbf{x}^{(j)}, \mathbf{h}) \right\|_2^2 \quad (51)$$

subject to

$$\|\mathbf{h}\|_2 \leq \delta^{(j)}. \quad (52)$$

Thus, the step taken is constrained by a suitable trust region $\delta^{(j)}$. Solving (51) and (52) is equivalent to solving

$$(\mathbf{B}^{(j)T}\mathbf{B}^{(j)} + \lambda\mathbf{I})\mathbf{h}^{(j)} = -\mathbf{B}^{(j)T}\mathbf{f}^{(j)} \quad (53)$$

where $\mathbf{B}^{(j)}$ is an approximation to the Jacobian of the mapping \mathbf{P} at the j th iteration. The parameter λ can be selected such that the step is identical to that of (51). As in ASM, $\mathbf{B}^{(j)}$ is updated by Broyden's formula (18).

The trust-region ASM algorithm also uses recursive MPE (see Section V). Through the set of points used in the MPE, the algorithm estimates the Jacobian of the fine model.

C. Wedge Problem

A simple example illustrates the trust-region ASM algorithm. Consider a wedge that is required to be cut at a specific position so that the volume is equal to a specific value $V = 28$. The fine model is the wedge, as shown in Fig. 17(a). Observe that the coarse model is chosen to be uniformly cuboidal, as shown in Fig. 17(b). In this case, the coarse model volume is $R_c(x_c) = 2x_c$. The optimal coarse model solution is $x_c^* = 14$. Taking this as an initial value for the fine model $x_f^{(1)} = 14$, we evaluate the fine model response (volume) $R_f(x_f^{(1)}) = 43.75$. A PE step is applied to find the parameter that corresponds to a volume $V = 43.75$. We find that $x_c^{(1)} = 21.875$ and $f^{(1)} = 7.875$.

By solving the trust-region subproblem (51) and (52), taking $\mathbf{B}^{(1)} = 1$ and initial trust-region size $\delta^{(0)} = 2$, we find $\mathbf{h}^{(1)} = -2$. The next fine model iteration is $x_f^{(2)} = 12$. The fine model response at the current iteration is $R_f(x_f^{(2)}) = 39$. To evaluate how successful it is, another PE is required, which results in $x_c^{(2)} = 19.5$. It follows that $f^{(2)} = 5.5$ and using (49) to get $\rho = 1.1875$. Since $\rho > 1$, the current iteration is indicated as successful and the trust-region size is increased to, say, $\delta^{(1)} = 4$. The algorithm continues solving (51) and (52) to get $\mathbf{h}^{(2)} = -4$ and $x_f^{(3)} = 8$. Since $R_f(x_f^{(3)}) = 28$, the algorithm reaches the required optimum in two iterations (see Fig. 18). For other

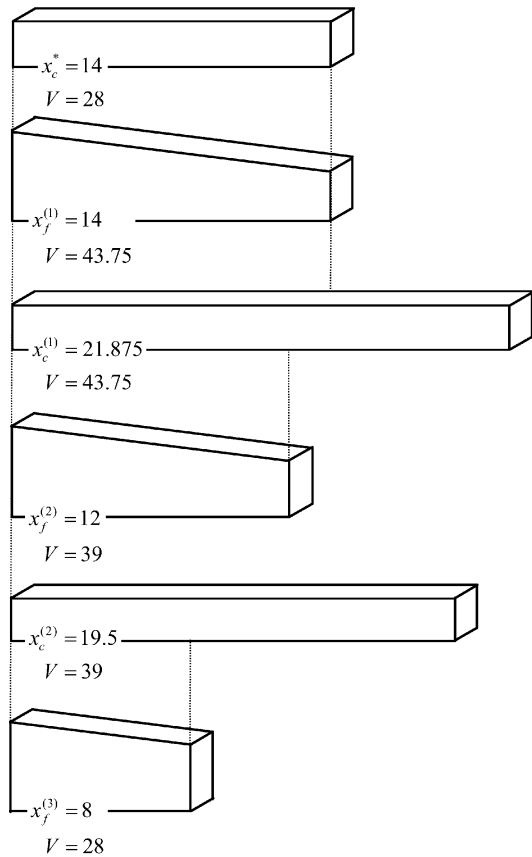


Fig. 18. Two iterations of a trust-region algorithm for the wedge problem.

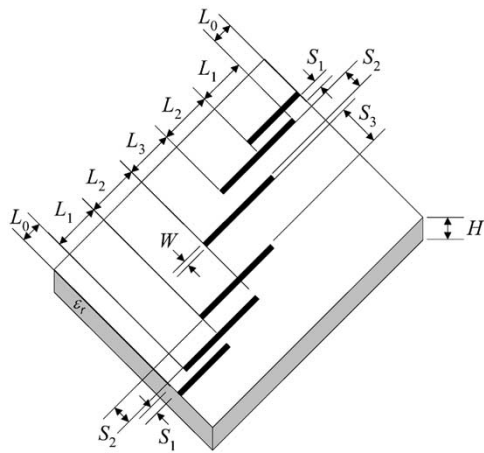


Fig. 19. HTS quarter-wave parallel coupled-line microstrip filter [15].

initial trust-region sizes, the process may take one or two more iterations.

D. High-Temperature Superconducting (HTS) Quarter-Wave Parallel Coupled-Line Microstrip Filter [5], [15], [16], [56]

Fig. 19 illustrates the structure of an HTS filter. $L_1, L_2,$ and L_3 are the lengths of the parallel coupled-line sections and $S_1, S_2,$ and S_3 are the gaps between the sections. The width W is the same for all the sections, as well as for the input and output MSLs, whose length is L_0 . A lanthanum aluminate substrate with thickness H and dielectric constant ϵ_r is used.

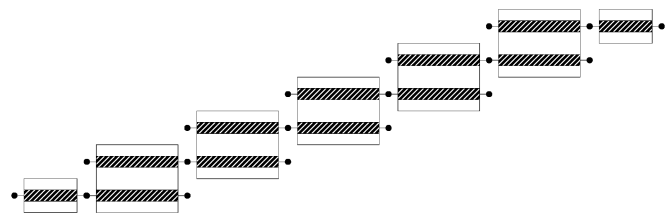


Fig. 20. Representation of the coarse model for the HTS microstrip filter [16].

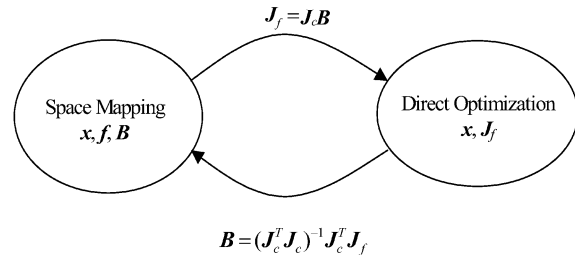


Fig. 21. Illustration of the connection between SM optimization and direct optimization or response matching.

The design parameters are $\mathbf{x}_f = [L_1 L_2 L_3 S_1 S_2 S_3]^T$. $L_0 = 50$ mil, $H = 20$ mil, $W = 7$ mil, $\epsilon_r = 23.425$, and loss tangent $= 3 \times 10^{-5}$; the metalization is considered lossless. The specifications are

$$\begin{aligned} |S_{21}| &\geq 0.95, & \text{for } 4.008 \text{ GHz} \leq \omega \leq 4.058 \text{ GHz} \\ |S_{21}| &\leq 0.05, & \text{for } \omega \leq 3.967 \text{ GHz and } \omega \geq 4.099 \text{ GHz.} \end{aligned}$$

It has been shown in [56] that the responses of this narrow bandwidth filter are very sensitive to dimensional changes.

The conceptual schematic of the coarse model used for the HTS filter is illustrated in Fig. 20. Built-in linear-element MSLs, two-conductor symmetrical coupled microstrip lines (MSCLs) and open circuit (OPEN) connected by circuit theory over the same microstrip substrate definition (MSUB) are taken as the “coarse” model.

Bakr *et al.* [12] optimized this HTS filter, where the coarse model exploits the empirical models of MSLs, coupled lines, and open stubs available in OSA90/hope. The fine model employs a fine-grid *em* simulation. The coarse model is optimized using the OSA90/hope minimax algorithm. The space-mapped fine model design was obtained in five iterations (eight fine model simulations).

VIII. HYBRID ASM AND SURROGATE-MODEL-BASED OPTIMIZATION

A. Hybrid ASM Algorithm [13]

Hybrid ASM starts with an SM optimization phase and defaults to a response matching phase when SM fails. The algorithm exploits (6) and (7) to enable switching between the two phases (see Fig. 21).

In the SM phase, trust-region ASM optimization is carried out using the objective function $\|\mathbf{f}\|_2^2$ for \mathbf{f} defined by (10). While in the response matching phase, the objective function is $\|\mathbf{g}\|_2^2$, where \mathbf{g} is defined by (8).

At the j th iteration, $\mathbf{x}_f^{(j+1)}$ is evaluated. If an actual reduction is achieved in $\|\mathbf{f}\|_2^2$ and $\|\mathbf{g}\|_2^2$, then the SM iteration is accepted,

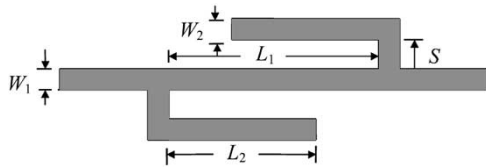


Fig. 22. DFS filter [4], [13].

the \mathbf{B} matrix is updated, and the SM optimization phase continues. Whenever no reduction is achieved in $\|\mathbf{g}\|_2^2$, the point $\mathbf{x}_f^{(j+1)}$ is rejected, the Jacobian of the fine model response $\mathbf{J}_f^{(j)}$ is evaluated at the point $\mathbf{x}_f^{(j)}$ using (6) and response matching starts.

If $\mathbf{x}_f^{(j+1)}$ achieves reduction in $\|\mathbf{g}\|_2^2$, but does not achieve any reduction in $\|\mathbf{f}\|_2^2$, mainly because of the PE nonuniqueness, the point $\mathbf{x}_f^{(j+1)}$ is accepted and recursive MPE is used to find another vector $\mathbf{f}^{(j+1)}$. If the new $\mathbf{f}^{(j+1)}$ still does not achieve improvement in $\|\mathbf{f}\|_2^2$, $\mathbf{J}_f^{(j+1)}$ is approximated using the $n + 1$ MPE fine model points, then $\mathbf{x}_f^{(j+1)}$ and $\mathbf{J}_f^{(j+1)}$ are supplied to the response matching phase.

B. Double-Folded-Stub (DFS) Filter [4], [9], [12], [13]

We consider the design of the DFS microstrip filter [4]. The filter is characterized by five parameters, i.e., W_1 , W_2 , S , L_1 , and L_2 (see Fig. 22). L_1 , L_2 , and S are chosen as optimization variables. W_1 and W_2 are fixed at 4.8 mil. The design specifications are

$$\begin{aligned} |S_{21}| &\geq -3 \text{ dB}, & \text{for } \omega \leq 9.5 \text{ GHz and } \omega \geq 16.5 \text{ GHz} \\ |S_{21}| &\leq -30 \text{ dB}, & \text{for } 12 \text{ GHz} \leq \omega \leq 14 \text{ GHz}. \end{aligned}$$

A coarse model (Fig. 23) exploits the MSL and microstrip T-junction models available in OSA90/hope. The coupling between the folded stubs and MSL is simulated using equivalent capacitors.

The fine model is simulated by HP HFSS⁴ through HP Empepe3D.⁵ The fine model response at \mathbf{x}_c^* is shown in Fig. 24. We see a big shift between the optimal coarse response and initial fine response. The first phase successfully carried out eight iterations (12 fine model simulations). Through (6), a mapping estimates \mathbf{J}_f and a switch to the second phase is carried out. The design at the end of the second phase is taken as the starting point for minimax optimization. The optimal response \mathbf{R}_f^* is shown in Fig. 25. The optimal designs are given in Table II.

C. Surrogate Model-Based SM Algorithm [14]

Surrogate model-based SM optimization exploits a surrogate in the form of a convex combination of a mapped coarse model and a linearized fine model. The algorithm employs the trust-region method in which the surrogate replaces the formal approx-

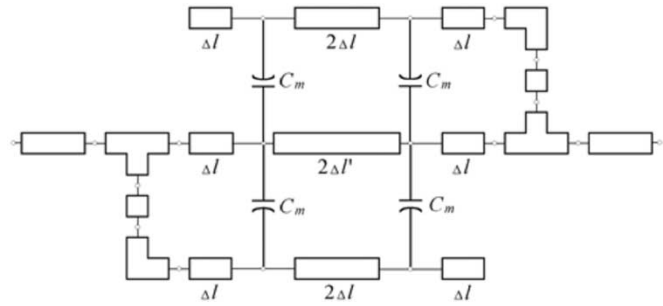


Fig. 23. Coarse model of the DFS filter [13].

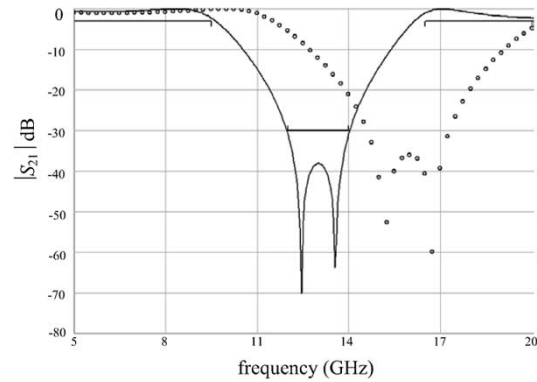
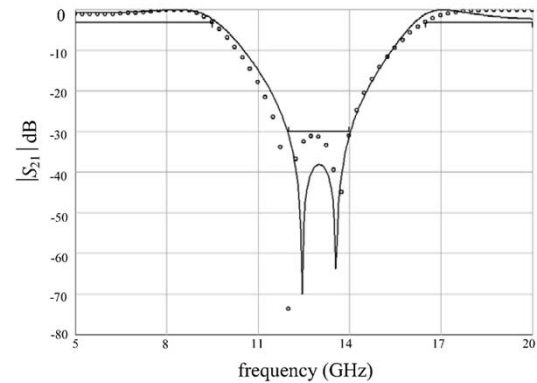
Fig. 24. Coarse response \mathbf{R}_c^* (—) and fine response $\mathbf{R}_f(\mathbf{x}_c^*)(\circ)$ for the DFS filter [13].Fig. 25. Coarse response \mathbf{R}_c^* (—) and fine response $\mathbf{R}_f(\circ)$ for the DFS filter [13].

TABLE II
OPTIMAL COARSE MODEL DESIGN AND OPTIMAL FINE MODEL DESIGN
FOR THE DFS FILTER [13]

Parameter	\mathbf{x}_c^*	\mathbf{x}_f^*
L_1	66.727	78.964
L_2	60.228	81.210
S	9.592	7.901
all values are in mil		

imation to a linear or quadratic model. At the j th iteration, the surrogate model response $\mathbf{R}_s^{(j)} \in \mathfrak{R}^{m \times 1}$ is given by

$$\mathbf{R}_s^{(j)}(\mathbf{x}_f) \triangleq \lambda^{(j)} \mathbf{R}_m^{(j)}(\mathbf{x}_f) + (1 - \lambda^{(j)}) \left(\mathbf{R}_f(\mathbf{x}_f^{(j)}) + \mathbf{J}_f^{(j)} \Delta \mathbf{x}_f \right) \quad (54)$$

⁴HP HFSS, version 5.2, EEsof Division Hewlett-Packard Corporation, Santa Rosa, CA, 1998.

⁵HP Empepe3D, version 5.2, EEsof Division, Hewlett-Packard Corporation, Santa Rosa, CA, 1998.

where $\mathbf{R}_m^{(j)}(\mathbf{x}_f)$ is the mapped coarse model response, $\mathbf{R}_f^{(j)} + \mathbf{J}_f^{(j)} \Delta \mathbf{x}_f$ is the linearized fine model response, and $\lambda^{(j)}$ is a parameter to determine how each model is favored. If $\lambda^{(j)} = 1$, the surrogate becomes a mapped coarse model. If $\lambda^{(j)} = 0$, the surrogate becomes a linearized fine model. Initially, $\lambda^{(0)} = 1$. Its update at each iteration depends on the predicted errors produced by the mapped coarse model and the linearized fine model with respect to the fine model [14].

The step suggested is given by

$$\mathbf{h}^{(j)} = \arg \min_{\mathbf{h}} U \left(\mathbf{R}_s^{(j)}(\mathbf{x}_f^{(j)} + \mathbf{h}) \right) \quad (55)$$

$$\|\mathbf{h}\| \leq \delta^{(j)}$$

where $\delta^{(j)}$ is the trust-region size at the j th iteration. The mapped coarse model utilizes a frequency-sensitive mapping. This idea is covered in Section X.

Two approaches based on (54) are described in [28] and [31]. In [28], the value of $\lambda^{(j)}$ is monotonically decreased from 1 to 0 during the iterations. In [14], the value of $\lambda^{(j)}$ is only decreased if unsuccessful steps are produced. In [31], $\lambda^{(j)} = 1$ until at least n linearly independent steps have been tried. Thereafter, $\lambda^{(j)}$ remains one until an unsuccessful step is produced, then $\lambda^{(j)}$ is set to zero for the remaining iterations.

The surrogate model-based SM algorithm has been illustrated through the design of microwave filters and transformers [14]. For the HTS filter described in Section VII, the fine model is simulated at 16 frequency points per sweep. Starting from the optimal coarse model design, a total of seven fine model simulations are required to reach the final design.

IX. ISM

ISM [19] is a recent development. Selected preassigned parameters are extracted to match the coarse and fine models. Examples of preassigned parameters are dielectric constant and substrate height. With these parameters fixed, the calibrated coarse model (the surrogate) is reoptimized. The optimized parameters are assigned to the fine model. This process repeats until the fine model response is sufficiently close to the target response.

The idea of using preassigned parameters was introduced in [57] within an expanded SM design framework. This method selects certain key preassigned parameters based on sensitivity analysis of the coarse model. These parameters are extracted to match corresponding coarse and fine models. A mapping from optimization parameters to preassigned parameters is then established.

As indicated in Fig. 26, ISM aims at establishing an implicit mapping \mathbf{Q} between the spaces \mathbf{x}_f , \mathbf{x}_c , and \mathbf{x}

$$\mathbf{Q}(\mathbf{x}_f, \mathbf{x}_c, \mathbf{x}) = \mathbf{0} \quad (56)$$

where \mathbf{x} is a set of auxiliary parameters, e.g., preassigned, to be varied in the coarse model only. Thus, the corresponding calibrated coarse model (surrogate) response is $\mathbf{R}_c(\mathbf{x}_c, \mathbf{x})$.

ISM optimization obtains a space-mapped design $\bar{\mathbf{x}}_f$ whose response approximates an optimized \mathbf{R}_c target. It is a solution of the nonlinear system (56), obtained through a PE with respect to \mathbf{x} and (re)optimization of the surrogate with respect to \mathbf{x}_c to

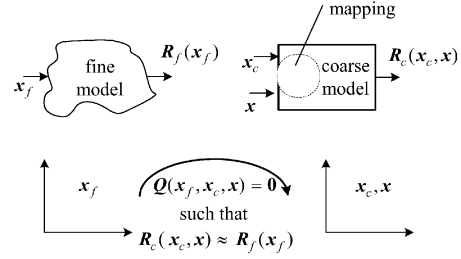


Fig. 26. Illustration of the ISM concept.

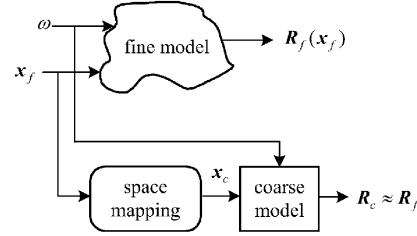


Fig. 27. SM super-model concept [21].

give $\bar{\mathbf{x}}_f = \mathbf{x}_c^*(\mathbf{x})$, the prediction of the fine model. The corresponding response is denoted \mathbf{R}_c^* .

ISM is effective for microwave circuit modeling and design using full-wave EM simulators. Since explicit mapping is not involved, this “SM” technique is more easily implemented than [57]. The HTS filter design is entirely done by Agilent ADS⁶ and Momentum⁷ or Sonnet’s *em*, with no matrices to keep track of.

X. SM-BASED MODEL ENHANCEMENT

The development of fast accurate models for components that can be utilized for CAD over wide ranges of the parameter space is crucial [15], [21], [22], [58]. Consider

$$\mathbf{R}_f(\mathbf{x}_f, \omega) \approx \mathbf{R}_c(\mathbf{P}(\mathbf{x}_f, \omega)). \quad (57)$$

This formulation offers the possibility of enhancing a pre-existing coarse model through mapping. Approaches to SM-based model enhancement differ in the way in which the mapping is established, the nature of the mapping, and the region of validity. The generalized SM tableau approach, space derivative mapping approach, and SM-based neuromodeling have been proposed. Here, we review the first two. The third one is covered in Section XI.

A. GSM Tableau [21]

This engineering device modeling framework exploits the SM [4], frequency SM [5], and multiple SM [59] concepts.

Three cases are reviewed. The SM super model (Fig. 27) uses only designable device parameters. The frequency-SM super model (Fig. 28) maps frequency as well as designable device parameters. In multiple SM, either the device responses or the frequency intervals are divided into a number of subsets and a separate mapping is established for each.

⁶Agilent ADS, version 1.5, Agilent Technol., Santa Rosa, CA, 2000.

⁷Agilent Momentum, version 4.0, Agilent Technol., Santa Rosa, CA, 2000.

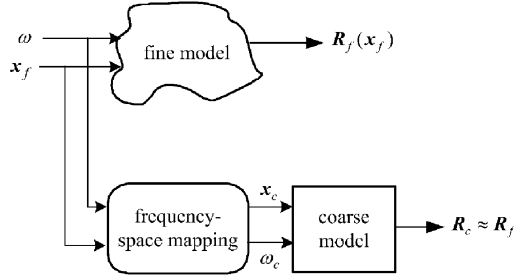


Fig. 28. Frequency-SM super-model concept [21].

B. Mathematical Formulation for GSM

The mapping relating fine model parameters and frequency to coarse model parameters and frequency is given by

$$(\mathbf{x}_c, \omega_c) = \mathbf{P}(\mathbf{x}_f, \omega). \quad (58)$$

or, in matrix form, assuming a linear mapping,

$$\begin{bmatrix} \mathbf{x}_c \\ \omega_c^{-1} \end{bmatrix} = \begin{bmatrix} \mathbf{c} \\ \delta \end{bmatrix} + \begin{bmatrix} \mathbf{B} & \mathbf{s} \\ \mathbf{t}^T & \sigma \end{bmatrix} \begin{bmatrix} \mathbf{x}_f \\ \omega^{-1} \end{bmatrix}. \quad (59)$$

The parameters $\{\mathbf{c}, \mathbf{B}, \mathbf{s}, \delta, \mathbf{t}, \sigma\}$ can be evaluated, directly or indirectly, by solving the optimization problem

$$\min_{\mathbf{c}, \mathbf{B}, \mathbf{s}, \delta, \mathbf{t}, \sigma} \left\| \begin{bmatrix} \mathbf{e}_1^T & \mathbf{e}_2^T & \cdots & \mathbf{e}_N^T \end{bmatrix}^T \right\| \quad (60)$$

where N is the number of the fine model simulations and \mathbf{e}_k is an error vector given by

$$\mathbf{e}_k = \mathbf{R}_f(\mathbf{x}_{f_i}, \omega_j) - \mathbf{R}_c(\mathbf{x}_c, \omega_c) \quad (61)$$

with $i = 1, \dots, B_p$ (the number of base points), $j = 1, \dots, F_p$ (the number of frequency points) and $k = j + (i - 1)F_p$. The total number of fine model simulations is $N = B_p F_p$.

The inverse of the frequency variable (proportional to wavelength) used (59) shows good results [21].

C. Microstrip Shaped T-Junction [21]

A shaped T-junction is shown in Fig. 29(a). This T-junction was introduced in [60] to compensate discontinuities. It is compared in [61] with the other T-junction configurations in the literature. The T-junction is symmetric in the sense that all input lines have the same width w elements [see Fig. 29(a)]. The design parameters are $\mathbf{x} = [w \ h \ w_1 \ w_2 \ x \ y \ \epsilon_r]^T$.

The region of interest is given in Table III. The frequency range is 2–20 GHz. The width w of the input lines is determined in terms of h and ϵ_r , so that the characteristic impedance of the input lines is 50 Ω .

The multiple SM for frequency intervals algorithm [21] was applied to enhance the accuracy of the T-junction coarse model. The fine model is analyzed by Sonnet's *em*. The coarse models [see Fig. 29(b)] are composed of empirical models of

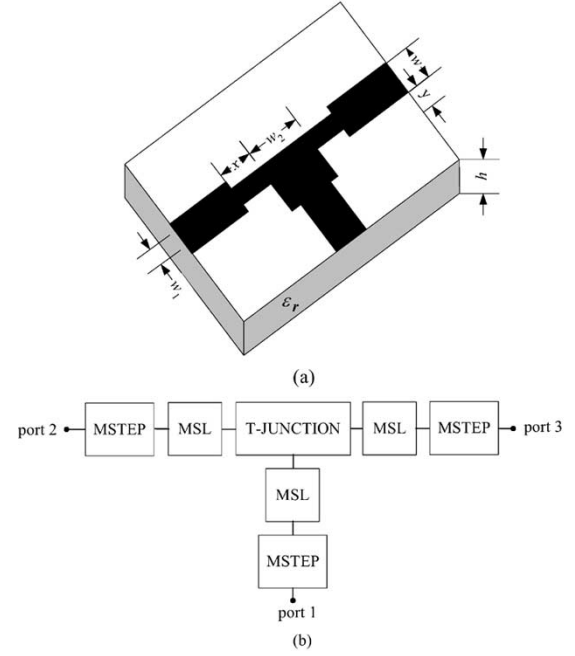


Fig. 29. Microstrip shaped T-junction. (a) Physical structure (fine model). (b) Coarse model [21].

TABLE III
REGION OF INTEREST FOR THE MICROSTRIP SHAPED T-JUNCTION [21]

Parameter	Minimum value	Maximum value
h	15 mil	25 mil
x	5 mil	15 mil
y	5 mil	15 mil
ϵ_r	8	10

microstrip elements of OSA90/hope. The algorithm divides the total frequency range into two intervals: 2–16 and 16–20 GHz. Table IV shows corresponding mapping parameters for each interval. Fig. 30 shows $|S_{11}|$ and $|S_{22}|$ at two test points in the region of interest.

The enhanced coarse model for the shaped T-junction is optimized to achieve the possible minimum mismatch at the three ports. The optimization variables are x and y , the other parameters w , h , and ϵ_r are kept fixed [61]. The specifications [61] are $|S_{11}| \leq 1/3$ and $|S_{22}| \leq 1/3$ in the range of 2–16 GHz. The minimax algorithm in OSA90/hope reached the solution $x = 2.1$ mil and $y = 21.1$ mil, which agrees with [61]. $|S_{11}|$ and $|S_{22}|$ are shown in Fig. 31.

D. Space Derivative Mapping [22]

This algorithm develops a locally valid approximation of the fine model in the vicinity of a particular point $\tilde{\mathbf{x}}_f$. We denote by $\tilde{\mathbf{J}}_f$ the Jacobian of the fine model responses at $\tilde{\mathbf{x}}_f$. The first step obtains the point $\tilde{\mathbf{x}}_c$ corresponding to $\tilde{\mathbf{x}}_f$ through the SPE problem (11). The Jacobian $\tilde{\mathbf{J}}_c$ at $\tilde{\mathbf{x}}_c$ may be estimated by finite differences. Both (11) and the evaluation of $\tilde{\mathbf{J}}_c$ should add no

TABLE IV
MAPPING PARAMETERS FOR THE MICROSTRIP SHAPED T-JUNCTION USING MULTIPLE SM FOR FREQUENCY INTERVALS [21]

	2 GHz to 16 GHz	16 GHz to 20 GHz
B	$\begin{bmatrix} 1.04 & 0.07 & 0.01 & 0.08 & -0.06 & 0.00 & 0.22 \\ 0.00 & 0.89 & 0.00 & -0.07 & -0.20 & 0.06 & -0.03 \\ -0.00 & 0.07 & 0.99 & 0.04 & -0.12 & 0.01 & -0.06 \\ -0.04 & 0.00 & -0.01 & 0.97 & 0.10 & -0.06 & -0.27 \\ 0.01 & 0.04 & 0.00 & 0.03 & 0.99 & -0.05 & -0.03 \\ -0.13 & -0.05 & -0.04 & -0.16 & 0.12 & 0.99 & 0.62 \\ -0.08 & 0.12 & -0.03 & 0.00 & -0.07 & 0.03 & 0.83 \end{bmatrix}$	$\begin{bmatrix} 0.99 & 0.02 & -0.00 & 0.01 & -0.09 & -0.01 & 0.13 \\ 0.05 & 0.85 & 0.01 & -0.07 & -0.28 & 0.01 & -0.01 \\ -0.06 & 0.15 & 0.98 & 0.04 & -0.25 & 0.00 & 0.02 \\ -0.10 & -0.06 & -0.03 & 0.88 & 0.13 & -0.09 & -0.27 \\ 0.08 & 0.04 & 0.03 & 0.11 & 1.07 & -0.04 & -0.12 \\ -0.14 & -0.02 & -0.05 & -0.15 & 0.23 & 1.03 & 0.51 \\ -0.13 & 0.22 & -0.04 & 0.02 & -0.07 & 0.03 & 0.87 \end{bmatrix}$
C	$[0.02 \ 0.01 \ -0.01 \ -0.03 \ -0.01 \ 0.07 \ -0.03]^T$	$[0.01 \ 0.01 \ -0.01 \ -0.03 \ -0.01 \ 0.05 \ -0.03]^T$
s	$[-0.01 \ 0.09 \ -0.10 \ -0.02 \ 0.00 \ -0.02 \ -0.20]^T$	$[0.00 \ 0.01 \ -0.01 \ 0.00 \ 0.00 \ 0.00 \ -0.02]^T$
t	$\mathbf{0}$	$[0.01 \ 0.00 \ -0.02 \ 0.00 \ 0.00 \ 0.00 \ 0.00]^T$
σ	0.851	0.957
δ	-0.003	0.008

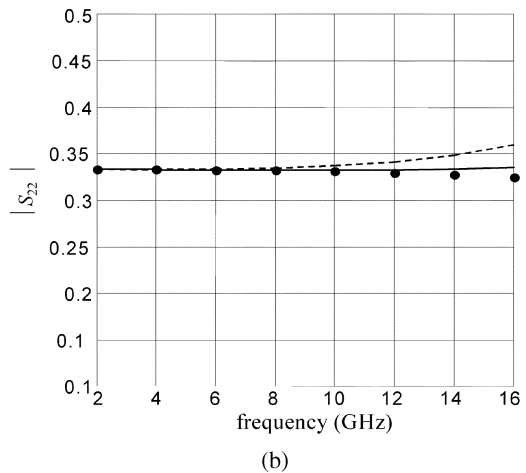
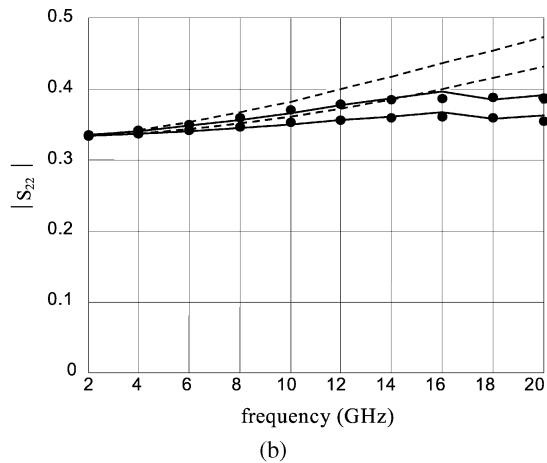
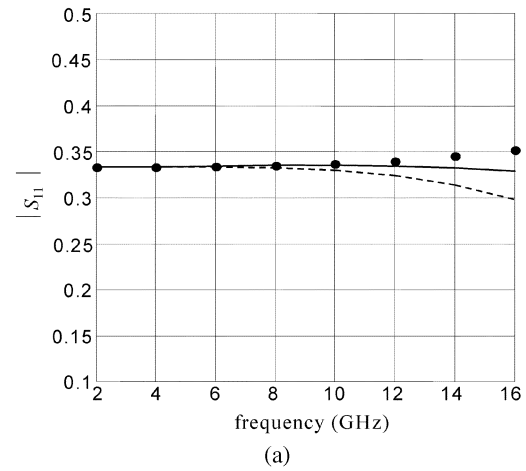
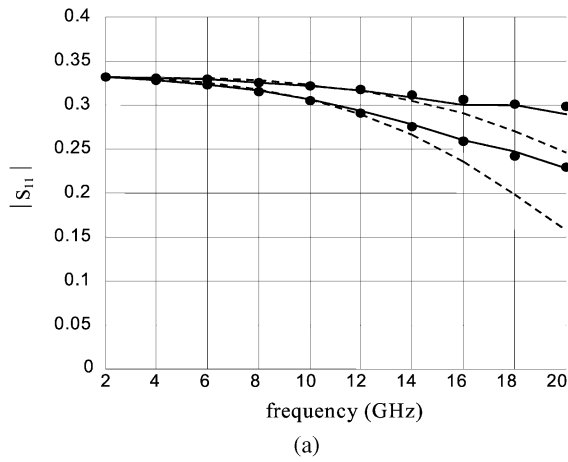


Fig. 30. Responses of the shaped T-junction at two test points in the region of interest by Sonnet's *em* (\bullet), by the coarse model (---), and by the enhanced coarse model (—). (a) $|S_{11}|$. (b) $|S_{22}|$ [21].

Fig. 31. Responses of the optimum shaped T-junction by Sonnet's *em* (\bullet), by the coarse model (---), and by the enhanced coarse model (—). (a) $|S_{11}|$. (b) $|S_{22}|$ [21].

significant overhead. The mapping matrix B is then calculated by applying (7) as

$$B = \left(\tilde{J}_c^T \tilde{J}_c \right)^{-1} \tilde{J}_c^T \tilde{J}_f. \quad (62)$$

Once B is available, the linear mapping is given by

$$\mathbf{x}_c = P(\mathbf{x}_f) \triangleq \tilde{\mathbf{x}}_c + B(\mathbf{x}_f - \tilde{\mathbf{x}}_f). \quad (63)$$

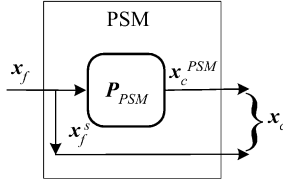


Fig. 32. PSM [10].

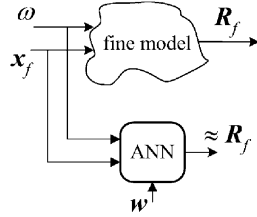


Fig. 33. Conventional neuromodeling approach [15].

The space derivative mapping model is given by (57) with P given by (63).

The space derivative mapping technique was applied to statistical analysis of a two-section waveguide impedance transformer and a six-section H -plane waveguide filter. For these examples, the statistical responses assumed the design parameters are uniformly distributed with relative tolerance.

E. Partial Space Mapping (PSM) and Derivative-Based SM [10]

Utilizing a reduced set of physical parameters of the coarse space might be sufficient to obtain an adequate surrogate. A selected set of design parameters are mapped onto the coarse space and the rest, i.e., $\mathbf{x}_f^s \subset \mathbf{x}_f$, are passed through unmapped. The mapped coarse parameters are denoted by $\mathbf{x}_c^{\text{PSM}} \in \mathfrak{R}^{k \times 1}$, $k \leq n$, where n is the number of design parameters. PSM is illustrated in Fig. 32. It can be represented in matrix form by

$$\mathbf{x}_c = \begin{bmatrix} \mathbf{x}_c^{\text{PSM}} \\ \mathbf{x}_f^s \end{bmatrix} = \begin{bmatrix} P_{\text{PSM}}(\mathbf{x}_f) \\ \mathbf{x}_f^s \end{bmatrix}. \quad (64)$$

In this context, (6) becomes

$$\mathbf{J}_f \approx \mathbf{J}_c^{\text{PSM}} \mathbf{B}^{\text{PSM}} \quad (65)$$

where $\mathbf{B}^{\text{PSM}} \in \mathfrak{R}^{k \times n}$ and $\mathbf{J}_c^{\text{PSM}} \in \mathfrak{R}^{m \times k}$ is the Jacobian of the coarse model at $\mathbf{x}_c^{\text{PSM}}$. Solving (65) for \mathbf{B}^{PSM} yields the least squares solution at the j th iteration

$$\mathbf{B}^{\text{PSM}(j)} = \left(\mathbf{J}_c^{\text{PSM}(j)T} \mathbf{J}_c^{\text{PSM}(j)} \right)^{-1} \mathbf{J}_c^{\text{PSM}(j)T} \mathbf{J}_f^{(j)}. \quad (66)$$

Relation (16) becomes underdetermined since \mathbf{B}^{PSM} is a rectangular matrix with the number of columns is greater than the number of rows. The minimum norm solution for $\mathbf{h}^{(j)}$ is

$$\mathbf{h}_{\text{min norm}}^{(j)} = \mathbf{B}^{\text{PSM}(j)T} \left(\mathbf{B}^{\text{PSM}(j)} \mathbf{B}^{\text{PSM}(j)T} \right)^{-1} \left(-\mathbf{f}^{(j)} \right). \quad (67)$$

The coarse model parameters $\mathbf{x}_c^{\text{PSM}}$ used in the PE can be determined by the sensitivity analysis proposed in [57].

XI. NEURAL SM

ANNs are suitable for modeling high-dimensional and highly nonlinear devices due to their ability to learn and generalize from data, their nonlinear processing nature, and their massively parallel structure [18].

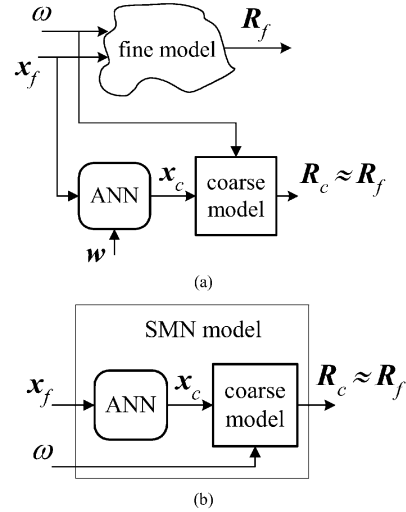


Fig. 34. Space-mapped neuromodeling (SMN). (a) SMN training. (b) SMN model [15].

In the conventional approach (Fig. 33), an ANN is trained such that it approximates \mathbf{R}_f in a region of interest for \mathbf{x}_f and operating frequency ω , where vector \mathbf{w} contains the internal parameters of the ANN (weighting factors, bias, etc.). Once the ANN is trained with sufficient learning samples, i.e., once the optimal \mathbf{w} is found, the ANN can be used as a fast and accurate model within the region of interest [62].

Strategies have been proposed to reduce the learning data and improve generalization capabilities of an ANN by incorporating empirical models or microwave knowledge [63]–[67]. Rayas-Sánchez reviews the state of the art in EM-based design and optimization of microwave circuits using ANNs [68].

A. SM-Based Neuromodeling [15]

Using an ANN, a mapping P from the fine to the coarse input space is constructed. The implicit “expert” knowledge in the coarse model permits a reduced number of learning points and reduces complexity of the ANN (Fig. 34).

Here, we solve the optimization problem

$$\min_{\mathbf{w}} \left\| \left[\mathbf{e}_1^T \quad \mathbf{e}_2^T \quad \cdots \quad \mathbf{e}_l^T \right]^T \right\| \quad (68)$$

where l is the total number of learning samples and \mathbf{e}_k is the error vector given by

$$\mathbf{e}_k(\mathbf{w}) \triangleq \mathbf{R}_f(\mathbf{x}_{f_i}, \omega_j) - \mathbf{R}_c(P(\mathbf{x}_{f_i}, \mathbf{w}), \omega_j) \quad (69)$$

with $i = 1, \dots, B_p$ being the number of base points, $j = 1, \dots, F_p$ being the number of frequency points, and $k = j + (i-1)F_p$ (see Section X). A star set for the base learning points (Fig. 35) is considered. A Huber norm is used in (68), exploiting its robust characteristics for data fitting [69].

Frequency-sensitive mappings from the fine to the coarse spaces can be realized by making frequency an additional input variable of the ANN that implements the mapping [15].

B. NSM [16]

A strategy is proposed to exploit the SM-based neuromodeling techniques [15] in an optimization algorithm, including frequency mapping (Fig. 36). A coarse model is used to select the initial learning base points through sensitivity analysis.

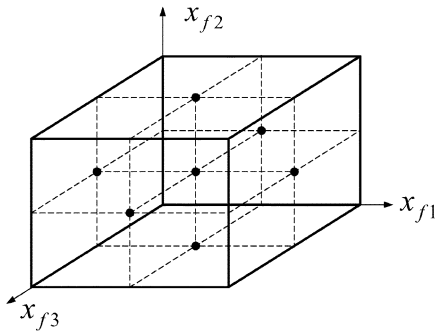


Fig. 35. 3-D star set for the learning base points [15].

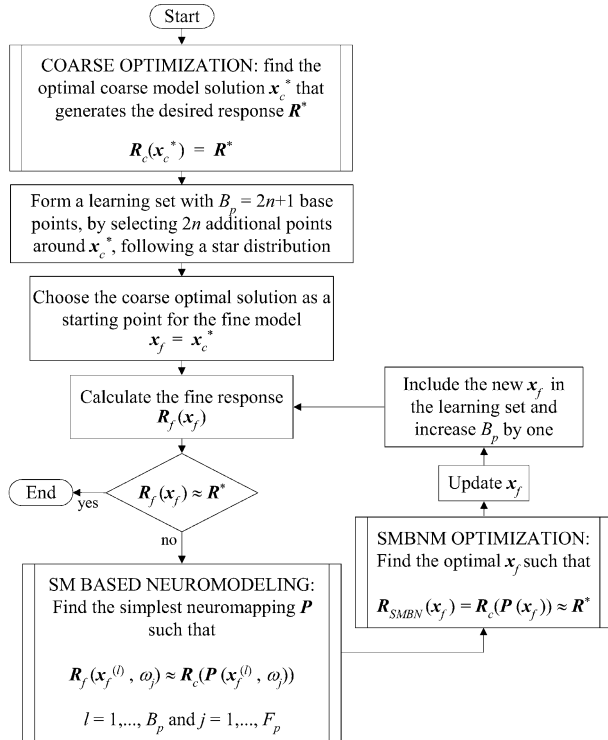


Fig. 36. NSM optimization [16]. The coarse and fine model design parameters are denoted by \mathbf{x}_c and $\mathbf{x}_f \in \mathfrak{R}^{n \times 1}$, respectively. The corresponding response vectors are denoted by \mathbf{R}_c and $\mathbf{R}_f \in \mathfrak{R}^{m \times 1}$, respectively. The optimal coarse model response \mathbf{R}^* is the target response. The number of base points is B_p , and $\mathbf{x}_f^{(l)}$ is the l th base point. The number of frequency points is F_p , and ω_j is the j th frequency point. The total number of fine model simulations is $N = B_p F_p$.

The proposed procedure does not require PE to predict the next point. Huber optimization is used to train the SM-based neuromodels at each iteration. These neuromodels are developed without using testing points: their generalization performance is controlled by gradually increasing their complexity starting with a three-layer perceptron with zero hidden neurons. Five neuromapping variations have been presented [16].

C. NISM [17]

NISM follows the aggressive approach [5] by not requiring a number of up-front fine model evaluations to start building the mapping. A statistical procedure for PE is used to overcome poor local minima. At each iteration, a neural network whose generalization performance is controlled through a network growing strategy approximates the inverse of the mapping. The NISM step simply evaluates the current neural net-

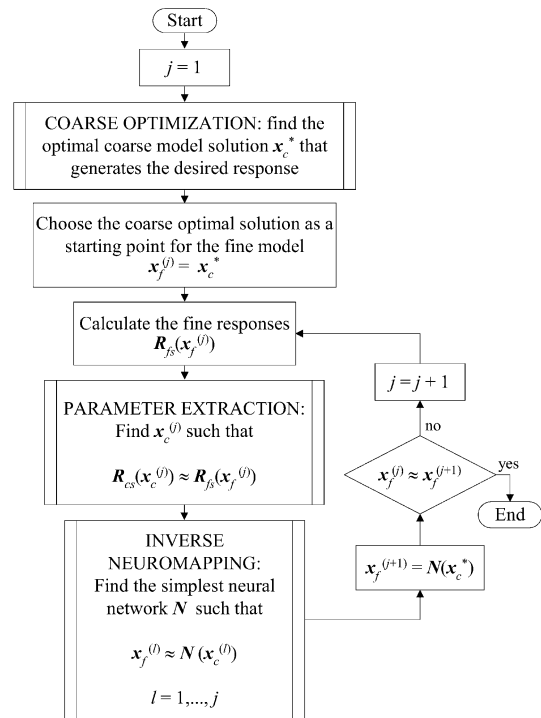


Fig. 37. NISM optimization [17]. The coarse and fine model design parameters are denoted by \mathbf{x}_c and $\mathbf{x}_f \in \mathfrak{R}^{n \times 1}$, respectively. \mathbf{R}_{cs} and \mathbf{R}_{fs} are the coarse and fine model characterizing responses for PE, respectively. \mathbf{x}_c^* is the optimal coarse model point. The inverse mapping between \mathbf{x}_c and \mathbf{x}_f is created by the simplest neural network N .

work at the optimal coarse solution. This step is equivalent to a quasi-Newton step, while the inverse mapping remains essentially linear. A flow diagram for the algorithm is shown in Fig. 37.

D. Yield Analysis and Yield Optimization [70]

Statistical simulation and yield optimization are essential to manufacturability-driven design. EM-based yield optimization requires intensive simulations to cover the entire statistic of possible outcomes of a given manufacturing process. This makes SM-based neuromodels, obtained either through modeling [15] or optimization [16] processes, attractive. This technique has increased the yield of an HTS filter from 14% to 69% [70]. In addition, excellent agreement is achieved between the SM-based neuromodel and the EM responses at the optimal yield solution.

XII. IMPLEMENTATION AND APPLICATIONS

A. RF and Microwave Implementation

The required interaction between coarse model, fine model, and optimization tools makes SM difficult to automate within existing simulators. A set of design or preassigned parameters and frequencies have to be sent to the different simulators and corresponding responses retrieved. Software packages such as OSA90 or MATLAB can provide coarse model analyses, as well as optimization tools. Empipe and Momentum driver [27] have been designed to drive and communicate with Sonnet's *em* and Agilent Momentum as fine models. ASM optimization of three-dimensional (3-D) structures [6] has been automated using a two-level Datapipe architecture of OSA90. The Datapipe technique allows the algorithm to carry

out nested optimization loops in two separate processes while maintaining a functional link between their results (e.g., the next increment to \mathbf{x}_f is a function of the result of PE).

Agilent ADS circuit models can be used as coarse models. ADS has a suite of built-in optimization tools. The ADS component S -parameter file enables S -parameters to be imported in Touchstone file format from different EM simulators (fine model) such as Sonnet's *em* and Agilent Momentum. Imported S -parameters can be matched with the ADS circuit model (coarse model) responses. This PE procedure can be done simply by proper setup of the ADS optimization components (optimization algorithm and goals). These major steps of SM are friendly for engineers to apply.

The object-oriented SMX [20] optimization system implements the surrogate model-based SM algorithm [14], which is automated for the first time. SMX has been linked with Empipe and Momentum driver to drive Sonnet's *em* and Agilent Momentum, as well as with user-defined simulators.

B. Structural Design [71]

Leary *et al.* apply the SM technique in civil engineering structural design. Their aim is to establish a mapping between the constraints of a fine model and coarse model. They illustrate their approach with a simple structural problem of minimizing the weight of a beam subject to constraints such as stress. Two models with different mesh densities are taken as fine and coarse models. The dimensions of the beam are optimization parameters. They found that the mapped model exhibited good agreement with the fine model with considerable reduction in the CPU effort.

C. Vehicle Crashworthiness Design [72], [73]

Redhe *et al.* [73] apply the SM technique and surrogate models together with response surfaces to structural optimization of crashworthiness problems. In crashworthiness problems, the intrusion into the passenger compartment is constrained. To construct the response surfaces, several computationally expensive function evaluations must be performed. A surrogate (coarse model) determines these surfaces and their associated gradients. Surrogates can be constructed using coarse meshes, simplified theoretical models or approximate analytic solutions. The full (fine) model finite-element method (FEM) simulator is used to correct the gradients for the next iteration. The fine model is evaluated once per iteration, then the results are added to the coarse model for response surface updating. Using the SM technique, CPU time is reduced relative to the traditional response surface methodology.

D. Automatic Model Generation, Neural Networks, and SM [74]

Devabhaktuni *et al.* propose a technique for generating microwave neural models of high accuracy using less accurate data. The proposed knowledge-based automatic model generation (KAMG) technique integrates automatic model generation, knowledge neural networks, and SM. The KAMG exploits fine data generators that are accurate and slow (e.g., CPU-intensive 3-D EM simulators) and coarse data generators that are approximate and fast (e.g., inexpensive two-dimensional (2-D) EM).

During neural model generation by KAMG, the intent is to make extensive use of the coarse generator and minimal use of the fine generator.

E. Combine Filter Design [75]

Combine-type microwave filters have found extensive applications as a result of their compact size, low cost, wide tuning range, and high performance. Swanson and Wenzel [75] introduce a design approach based on the SM concept and commercial FEM solvers. Their coarse model, generated by the CLD⁸ program, is a circuit model with an empirical correction for tap positions and gaps between rods. The fine model is analyzed by Agilent HFSS.⁹ Mechanical details such as finite radius can be added. S -parameters are obtained at the tuning screw locations by adding ports at these locations in the fine model. The entire filter can then be tuned using lumped capacitors in the circuit model. For a good starting point, one iteration is needed to implement the design process.

F. SM Implementation of Harscher *et al.* [76]

This technique combines EM simulations with a minimum prototype filter network (surrogate). They execute optimization in the surrogate model space with $n + 1$ EM simulations (in the best case), where n is the number of geometrical parameters.

Harscher *et al.* begin with an initial nonideal design for the EM model, then PE is performed. They obtain the filter characteristics, e.g., frequency shifts and coupling between resonators, sensitivities with respect to geometrical parameters by finite-difference approximations (n EM simulations). The ideal characteristic filter parameters are determined using filter synthesis, then the surrogate parameters are obtained through optimization exploiting sensitivities. Results are validated by an EM solver. If the specified target is not met, the PE step is used to start a new iteration. They present two examples: a direct coupled four-resonator E -plane filter and a dual-mode filter. The EM solver is based on mode matching.

G. CAD of Integrated Passive Elements on Printed Circuit Boards (PCBs) [77]

Draxler introduces a methodology for CAD of integrated passive elements on PCB incorporating surface mount technology (SMT). The proposed methodology uses the SM concept to exploit the benefits of both domains.

Parametric sub-networks (PSNs) have representations in the design phase (with SMT components) and the production phase (with PCB integrated passive components). The creation of the PSN reduces the risk of redesign. Draxler [77] defines an automated CAD structure that exploits a rapid component realization over multiple material specifications through mapping. The proposed approach enables component transformations between the two material domains.

Draxler [77] utilizes SM to create companion models by identifying which integrated passive physical parameters most closely match the SMT electrical behavior. A CAD process incorporating this feature could provide an SMT-PCB design

⁸CLD-Combine Design, version 3.0, Bartely R.F. Syst., Amesbury, MA, 2001.

⁹Agilent HFSS, version 5.6, Agilent EEsoft EDA, Santa Rosa, CA, 2000.

that exhibits the benefits of integrated passives with minimal risk of redesign [77].

H. CAD Technique for Microstrip Filter Design [78]

Ye and Mansour apply SM steps to reduce the simulation overhead required in microstrip filter design. They use a coarse model of cascaded microstrip circuit sections simulated individually by their EM simulator. Circuit components are used to account for the interaction between nonadjacent sections. These circuit components are determined with a few complete EM simulations. The coarse model is optimized at each iterate and the results verified by full EM simulation of the circuit. They illustrated their technique through an HTS filter.

I. SM Models for RF Components [79]

Snel [79] proposed the SM technique in RF filter design for power amplifier circuits. He suggests building a library of fast space-mapped RF filter components. These components can be incorporated in the design of ceramic multilayer filters for different center frequencies in wireless communication systems. The library is implemented in the Agilent ADS design framework.

J. Multilayer Microwave Circuits [Low-Temperature Co-Fired Ceramic (LTCC)] [80]

Pavio *et al.* apply typical SM techniques in optimization of high-density multilayer RF and microwave circuits. Initially, a “companion” or coarse model is optimized. The optimized circuit values are fed into the EM simulator. A PE step obtains the circuit values that match the EM simulation. The resulting change in coarse model parameters is directly applied (unity mapping, $\mathbf{B} = \mathbf{I}$) to the EM simulator for the next iteration. They suggest decomposition in developing coarse models for complex structures. They apply the SM approach to a three-pole bandstop filter LTCC capacitor, LTCC three-section bandstop filter, and an LTCC broad-band tapered transformer.

K. Cellular Power Amplifier Output Matching Circuit [81]

Lobeek [81] demonstrates the design of a digital communications system (DCS)/personal communications system (PCS) output match of a cellular power amplifier using SM. The design uses different technologies on a multilayer substrate carrier, which makes it difficult or even impossible to optimize the complete circuit of the output match. The design uses a six-layer LTCC substrate, a silicon passive integration die, discrete surface mount designs, as well as bond wires. Lobeek derives an SM model for the silicon passive integration die to integrate capacitors and low-value inductors. He optimizes the overall circuit to sufficient accuracy with this model.

Lobeek also applies the SM model to monitor the statistical behavior of the design with respect to parameter values. He uses nominal and yield optimization powered by SM and sensitivity analysis to create a manufacturable design. Monte Carlo analysis with EM accuracy based on the space-mapped model shows good agreement with manufactured data.

L. Multilevel Design Optimization Strategy [82]

Safavi-Naeini *et al.* consider a three-level design methodology for complex RF/microwave structure using an SM concept. They propose a circuit (coarse) model, an approximate (corrected quasi-static) model, and an EM (fine) model. The intermediate model maps the circuit model parameters to the corresponding physical parameters in the EM solver. They consider this a two-level SM. Their technique is implemented in the *WATML-MICAD* software. Applications include a parallel-coupled line filter, combline-type filters, and multiple-coupled cavity filters.

M. Coupled Resonator Filter [83]

Pelz applies SM in realization of narrow-band coupled resonator filter structures. A realization of such a filter involves the determination of dimensions of the apertures between the resonators. He considers a 3-D EM model as fine model and an equivalent *LC*-network model as the coarse model. A PE process obtains the coupling matrix of the *LC* network corresponding to the physical (EM) model parameters. A five-pole coupled resonator filter design is achieved with fast convergence.

N. LTCC RF Passive Circuits Design [84]

Wu *et al.* apply the ASM approach to LTCC RF passive circuit design. A third intermediate space called the “buffer knowledge” space, based on CAD formulas (knowledge), is introduced between the “fine” and “coarse” spaces. The reason for introducing this space is to link the physical parameters in the coarse and fine spaces (number of parameters can be different). We can view the coarse model in combination with the knowledge embedded space as an enhanced coarse model or surrogate well aligned with the fine model. They design LTCC 3-D multilayer structures used in wireless applications, e.g., W-CDMA bandpass filter.

O. Waveguide Filter Design [85]

Steyn *et al.* consider the design of irises in multimode coupled cavity filters. They combine a reduced generalized scattering matrix with ASM. Their aim is to reduce the number of EM analyses. In the design process, the optimization of an iris for specific coupling coefficients at a specific frequency requires roughly 35 coupling coefficient with eight EM evaluations per coupling coefficient to achieve max error of 0.01%. With the ASM technique, only four coupling coefficients were sufficient to obtain the same error.

P. Inductively Coupled Filters [86], [87]

Soto *et al.* and Morro *et al.* apply the ASM procedure to build a fully automated design of inductively coupled rectangular waveguide filters. A modal method based on the generalized admittance matrix is employed for both the fine and coarse models. The coarse model utilizes a smaller number of modes, while higher modes are incorporated in the fine model. Soto *et al.* incorporate a segmentation (decomposition) technique in the PE phase. They design two bandpass inductively coupled filters, with electrical responses centered at 11 and 13 GHz. The complete ASM design procedure required three iterations to con-

verge (ten times faster than directly using a precise simulation tool).

Q. Magnetic Systems [88]

The magnetic equivalent circuit (MEC) method and the FEM have been widely used for simulation of EM systems. The MEC method is computationally efficient, but lacks accuracy. The FEM is accurate, but relatively complex and computationally intensive [88]. Choi *et al.* utilize SM to design magnetic systems. The FEM model is the fine model and the MEC model with a closed form of lumped parameters is the coarse model. They validate the approach by two numerical examples, i.e., a magnetic device with leakage flux and a machine with highly saturated part. Both examples converge after only five iterations [88].

R. Dielectric Resonator Multiplexer Design [89]

Ismail *et al.* apply SM optimization with the FEM (fine model) to design a five-pole dielectric resonator loaded filter and a ten-channel output multiplexer. The coarse model of the filter uses a coupling matrix representation. The fine model includes tuning screws. The proposed approach reduces overall tuning time compared with traditional techniques.

S. Nonlinear Device Modeling [90]

Zhang *et al.* introduce a new neuro-SM approach for nonlinear device modeling and large-signal circuit simulation. A neural-network maps the current and voltage signals between the coarse and fine device models. By automatically modifying the voltage and current signals fed to the model using neuro-SM, the mapped model accurately matches the actual device behavior. The neuro-SM approach is demonstrated by modeling the SiGe HBT and GaAs field-effect transistor (FET) devices.

XIII. DISCUSSION OF SURROGATE MODELING AND SM

Table V lists a glossary of terms that is helpful in this discussion.

A. Building and Using Surrogates [91]

In his summarizing comments [91] on the Workshop on Surrogate Modelling and Space Mapping,¹⁰ Dennis integrates the terminology “coarse” and “fine” from the SM community with his own. Dennis uses the term “surrogate” to denote the function s to which an optimization routine is applied in lieu of applying optimization to the fine model f . Another piece of terminology he uses is “surface” to denote a function (it may be vector valued) trained to fit or to smooth fine model data.

Dennis mentions several ways to choose fine model data sites, also known as experimental designs. The surfaces are generated from the data sites. He notes that “surfaces (are) designed to correct a coarse model and to be combined with the coarse model to act as a surrogate in optimization.” He then used the surface concept to interpret SM. Here, “The surrogate is the coarse model

TABLE V
GLOSSARY OF TERMS

Term	Interpretation
Space Mapping	Intelligently links companion “coarse” and “fine” models: full-wave electromagnetic (EM) simulations and empirical models
Space Mapping	optimization follows traditional experience of designers
Space Mapping	an algorithm to enhance a coarse model to act as a surrogate
Space Mapping	surface, defined by Dennis [91]
Coarse Model	simplification or convenient representation, companion to the fine model, auxiliary representation, cheap model
Fine Model	accurate representation of system considered, device under test, component to be optimized, expensive model
Surrogate	model, approximation or representation to be used, or to act, in place of, or as a substitute for, the system under consideration
Surrogate	enhanced, aligned, mapped, calibrated (in each iteration) or combined model, always updated by the SM algorithm
Surrogate Model	alternative expression for (updated) coarse model
Target Response	response the fine model should achieve, (usually) optimal response of a coarse model, enhanced coarse model, or surrogate
Parameter (input) Space Mapping	mapping, transformation or correction of design variables
Response (output) Space Mapping	mapping, transformation or correction of responses
Response Surface Approximation	linear/quadratic/polynomial approximation of responses w.r.t. design variables
Neuro	Implies use of artificial neural networks
Implicit Space Mapping	space mapping when the mapping is not obvious
Not Space Mapping	might be space mapping, but unrecognized
Parameter Transformation	space mapping

applied to the image of the fine model parameters under the SM surface.”

Dennis discusses “heuristics” that optimize the surrogate and (perhaps) correct the surface part of the surrogate. He classifies SM in terms of “local SMs and methods that use poised designs implicitly or explicitly approximate derivatives. The former do this by Broyden updates and the latter by the derivatives of the surface.”

Dennis’s definition of surrogate agrees with our definition in the sense that the surrogate is an enhanced coarse model. Dennis regards the mapping as a surface.

We think of the mapping as that part of the surrogate, an approximation to which needs to be updated in each iteration. The mapping (surface) is the same during all iterations.

B. Building and Using Surrogates [92]

In an editorial, Bandler and Madsen emphasize that “surrogate optimization” refers to the process of applying an optimization routine directly to a coarse model, a surrogate, which is a

¹⁰First Int. Surrogate Modelling and Space Mapping for Engineering Optimization Workshop, Nov. 16–18, 2000. [Online]. Available: <http://www.imm.dtu.dk/~km/smsmeo/>

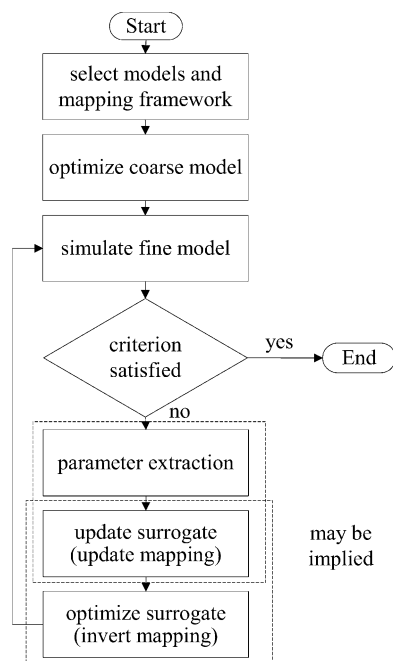


Fig. 38. General SM flowchart.

function (or a model) that replaces the original fine model. Some surrogates attempt to fit the fine model directly (e.g., by polynomials). In other cases, the information gained during the optimization process is used to train the surrogate to fit the data derived from evaluation of the fine model (e.g., by ANNs). In the SM approach, coarse models may be enhanced by mapping (transforming, correcting) the optimization variables. In this case, surrogates of increasing fidelity are developed during the optimization process.

C. SM Concept

All the SM-based optimization algorithms we review have four major steps. The first one is fine model simulation (verification). The fine model is verified and checked to see if it satisfies the design specifications. The second one is PE, in which the coarse model is (re)aligned with the fine model to permit (re)calibration. The third one is updating or (re)mapping the surrogate using the information obtained from the first two steps. At last the aligned, calibrated, mapped, or enhanced coarse model (the surrogate) is (re)optimized. This suggests a new fine model design iterate.

D. General SM Optimization Steps

A flowchart of general SM is shown in Fig. 38.

- Step 1) Select a coarse model suitable for the fine model.
- Step 2) Select a mapping process (original, ASM, neural, or ISM, etc.).
- Step 3) Optimize the coarse model (initial surrogate) with respect to design parameters.
- Step 4) Simulate the fine model at this solution.
- Step 5) Terminate if a stopping criterion is satisfied, e.g., response meets specifications.
- Step 6) Apply PE (neuron weights, coarse space design parameters).

Step 7) Rebuild surrogate (may be implied within Steps 6 or 8).

Step 8) Reoptimize the “mapped coarse model” (surrogate) with respect to design parameters (or evaluate the inverse mapping if it is available).

Step 9) Go to Step 4.

Comment: Rebuilding the surrogate (Step 7) may be implied in either the PE process (Step 6) or in the reoptimization (Step 8).

E. Output SM

Table V mentions “output” or response SM. This concept could address a residual misalignment in the optimal responses of the coarse and fine models. For example, a coarse model such as $R_c = x^2$ will never match the fine model $R_f = x^2 - 2$ around its minimum with any mapping $x_c = P(x_f)$, $x_c, x_f \in \mathfrak{R}$. An “output” or response mapping can overcome this deficiency by introducing a transformation of the coarse model response based on a Taylor approximation [93]. Current research is directed to this topic [94].

XIV. CONCLUSIONS

The SM technique and the SM-oriented surrogate (modeling) concept and their applications in engineering design optimization have been reviewed. The simple CAD methodology follows the traditional experience and intuition of engineers, yet appears to be amenable to rigorous mathematical treatment. The aim and advantages of SM are described. The general steps for building surrogates and SM are indicated. Proposed approaches to SM-based optimization include the original SM algorithm, the Broyden-based ASM, trust-region ASM, hybrid ASM, NSM, and ISM. PE is an essential subproblem of any SM optimization algorithm. It is used to align the surrogate with the fine model at each iteration. Different approaches to enhance the uniqueness of PE are reviewed, including the recent GPE process.

For the first time, we have presented a mathematical motivation for SM. We have placed SM into the context of classical optimization, which is based on local Taylor approximations. The SM model is seen as a good approximation over a large region, i.e., it is efficient in the initial phase when large iteration steps are needed, whereas the first-order Taylor model is better close to the solution.

Interesting SM and surrogate applications have been reviewed. They have indicated that exploitation of properly managed “space-mapped” surrogates promises significant efficiency in all branches of engineering design.

ACKNOWLEDGMENT

The authors thank J. C. Rautio, President, Sonnet Software Inc., Liverpool, NY, for making *em* available, and Agilent Technologies, Santa Rosa, CA, for ADS, Momentum, HFSS and HP Empipe3D. The authors also acknowledge the inspiring discussions with N. K. Nikolova, McMaster University, Hamilton, ON, Canada, F. Pedersen, Technical University of Denmark, Lyngby, Denmark, M. A. Ismail, ComDev International Ltd., Cambridge, ON, Canada, J. E. Rayas-Sánchez, Instituto Tecnológico y de Estudios Superiores de Occidente (ITESO), Tlaquepaque, Jalisco, Mexico, J. E. Dennis, Jr.,

Department of Computational and Applied Mathematics, Rice University, Houston, TX, and L. N. Vicente, Department of Mathematics, University of Coimbra, Coimbra, Portugal.

REFERENCES

- [1] M. B. Steer, J. W. Bandler, and C. M. Snowden, "Computer-aided design of RF and microwave circuits and systems," *IEEE Trans. Microwave Theory Tech.*, vol. 50, pp. 996–1005, Mar. 2002.
- [2] J. W. Bandler and S. H. Chen, "Circuit optimization: The state of the art," *IEEE Trans. Microwave Theory Tech.*, vol. 36, pp. 424–443, Feb. 1988.
- [3] J. W. Bandler, W. Kellermann, and K. Madsen, "A superlinearly convergent minimax algorithm for microwave circuit design," *IEEE Trans. Microwave Theory Tech.*, vol. MTT-33, pp. 1519–1530, Dec. 1985.
- [4] J. W. Bandler, R. M. Biernacki, S. H. Chen, P. A. Grobelny, and R. H. Hemmers, "Space mapping technique for electromagnetic optimization," *IEEE Trans. Microwave Theory Tech.*, vol. 42, pp. 2536–2544, Dec. 1994.
- [5] J. W. Bandler, R. M. Biernacki, S. H. Chen, R. H. Hemmers, and K. Madsen, "Electromagnetic optimization exploiting aggressive space mapping," *IEEE Trans. Microwave Theory Tech.*, vol. 43, pp. 2874–2882, Dec. 1995.
- [6] J. W. Bandler, R. M. Biernacki, and S. H. Chen, "Fully automated space mapping optimization of 3D structures," in *IEEE MTT-S Int. Microwave Symp. Dig.*, San Francisco, CA, 1996, pp. 753–756.
- [7] J. W. Bandler, R. M. Biernacki, S. H. Chen, and D. Omeragic, "Space mapping optimization of waveguide filters using finite element and mode-matching electromagnetic simulators," *Int. J. RF Microwave Computer-Aided Eng.*, vol. 9, pp. 54–70, 1999.
- [8] J. W. Bandler, R. M. Biernacki, S. H. Chen, and Y. F. Huang, "Design optimization of interdigital filters using aggressive space mapping and decomposition," *IEEE Trans. Microwave Theory Tech.*, vol. 45, pp. 761–769, May 1997.
- [9] M. H. Bakr, J. W. Bandler, and N. Georgieva, "An aggressive approach to parameter extraction," *IEEE Trans. Microwave Theory Tech.*, vol. 47, pp. 2428–2439, Dec. 1999.
- [10] J. W. Bandler, A. S. Mohamed, M. H. Bakr, K. Madsen, and J. Søndergaard, "EM-based optimization exploiting partial space mapping and exact sensitivities," *IEEE Trans. Microwave Theory Tech.*, vol. 50, pp. 2741–2750, Dec. 2002.
- [11] N. Alexandrov, J. E. Dennis, Jr., R. M. Lewis, and V. Torczon, "A trust region framework for managing the use of approximation models in optimization," *Structural Optimization*, vol. 15, pp. 16–23, 1998.
- [12] M. H. Bakr, J. W. Bandler, R. M. Biernacki, S. H. Chen, and K. Madsen, "A trust region aggressive space mapping algorithm for EM optimization," *IEEE Trans. Microwave Theory Tech.*, vol. 46, pp. 2412–2425, Dec. 1998.
- [13] M. H. Bakr, J. W. Bandler, N. K. Georgieva, and K. Madsen, "A hybrid aggressive space-mapping algorithm for EM optimization," *IEEE Trans. Microwave Theory Tech.*, vol. 47, pp. 2440–2449, Dec. 1999.
- [14] M. H. Bakr, J. W. Bandler, K. Madsen, J. E. Rayas-Sánchez, and J. Søndergaard, "Space mapping optimization of microwave circuits exploiting surrogate models," *IEEE Trans. Microwave Theory Tech.*, vol. 48, pp. 2297–2306, Dec. 2000.
- [15] J. W. Bandler, M. A. Ismail, J. E. Rayas-Sánchez, and Q. J. Zhang, "Neuromodeling of microwave circuits exploiting space mapping technology," *IEEE Trans. Microwave Theory Tech.*, vol. 47, pp. 2417–2427, Dec. 1999.
- [16] M. H. Bakr, J. W. Bandler, M. A. Ismail, J. E. Rayas-Sánchez, and Q. J. Zhang, "Neural space-mapping optimization for EM-based design," *IEEE Trans. Microwave Theory Tech.*, vol. 48, pp. 2307–2315, Dec. 2000.
- [17] J. W. Bandler, M. A. Ismail, J. E. Rayas-Sánchez, and Q. J. Zhang, "Neural inverse space mapping (NISM) optimization for EM-based microwave design," *Int. J. RF Microwave Computer-Aided Eng.*, vol. 13, pp. 136–147, 2003.
- [18] Q. J. Zhang and K. C. Gupta, *Neural Networks For RF and Microwave Design*. Norwood, MA: Artech House, 2000, ch. 9.
- [19] J. W. Bandler, Q. S. Cheng, N. K. Nikolova, and M. A. Ismail, "Implicit space mapping optimization exploiting preassigned parameters," *IEEE Trans. Microwave Theory Tech.*, vol. 52, pp. 378–385, Jan. 2004.
- [20] M. H. Bakr, J. W. Bandler, Q. S. Cheng, M. A. Ismail, and J. E. Rayas-Sánchez, "SMX—A novel object-oriented optimization system," in *IEEE MTT-S Int. Microwave Symp. Dig.*, Phoenix, AZ, 2001, pp. 2083–2086.
- [21] J. W. Bandler, N. Georgieva, M. A. Ismail, J. E. Rayas-Sánchez, and Q. J. Zhang, "A generalized space mapping tableau approach to device modeling," *IEEE Trans. Microwave Theory Tech.*, vol. 49, pp. 67–79, Jan. 2001.
- [22] M. H. Bakr, J. W. Bandler, and N. Georgieva, "Modeling of microwave circuits exploiting space derivative mapping," in *IEEE MTT-S Int. Microwave Symp. Dig.*, Anaheim, CA, 1999, pp. 715–718.
- [23] J.-S. Hong and M. J. Lancaster, *Microstrip Filters for RF/Microwave Applications*. New York: Wiley, 2001, pp. 295–299.
- [24] A. R. Conn, N. I. M. Gould, and P. L. Toint, *Trust-Region Methods*. Philadelphia, PA: SIAM, 2000, p. 11.
- [25] M. H. Bakr, "Advances in space mapping optimization of microwave circuits," Ph.D. dissertation, Dept. Elect. Comput. Eng., McMaster Univ., Hamilton, ON, Canada, 2000. [Online]. Available: http://www.sos.mcmaster.ca/theses/Bakr/Bakr_Thesis.pdf.
- [26] J. E. Rayas-Sánchez, "Neural space mapping methods for modeling and design of microwave circuits," Ph.D. dissertation, Dept. Elect. Comput. Eng., McMaster Univ., Hamilton, ON, Canada, 2001. [Online]. Available: http://www.sos.mcmaster.ca/theses/Rayas-Sanchez/jose_thesis.pdf.
- [27] M. A. Ismail, "Space mapping framework for modeling and design of microwave circuits," Ph.D. dissertation, Dept. Elect. Comput. Eng., McMaster University, Hamilton, ON, Canada, 2001. [Online]. Available: http://www.sos.mcmaster.ca/Theses/Ismail/Ismail_Thesis.pdf.
- [28] M. H. Bakr, J. W. Bandler, K. Madsen, and J. Søndergaard, "An introduction to the space mapping technique," *Optimization Eng.*, vol. 2, pp. 369–384, 2001.
- [29] J. Søndergaard, "Nonlinear optimization using space mapping," Masters thesis, Inform. Math. Modelling, Tech. Univ. Denmark, Lyngby, Denmark, 1999.
- [30] —, "Optimization using surrogate models—by the space mapping technique," Ph.D. dissertation, Inform. Math. Modelling, Tech. Univ. Denmark, Lyngby, Denmark, 2003. [Online]. Available: http://www.imm.dtu.dk/pubdb/views/publication_details.php?id=2450.
- [31] F. Pedersen, "Advances on the space mapping optimization method," Masters thesis, Inform. Math. Modelling, Tech. Univ. Denmark, Lyngby, Denmark, 2001. [Online]. Available: <http://www.byg.dtu.dk/cv-www/fp/publ/master/thesis.pdf>.
- [32] K. Madsen and J. Søndergaard, "Convergence of hybrid space mapping algorithms," *Optimization Eng.*, 2004, to be published.
- [33] L. N. Vicente, "Space mapping: Models, sensitivities, and trust-regions methods," presented at the SIAM Optimization in Engineering Design Conf. Workshop, Toronto, ON, Canada, 2002.
- [34] —, "Space mapping: Models, sensitivities, and trust-regions methods," *Optimization Eng.*, vol. 4, pp. 159–175, 2003.
- [35] —, "Space Mapping: Models, algorithms, and applications," Univ. Minnesota, Minneapolis, MN, <http://www.mat.uc.pt/~lrv/talks/imas-m2.pdf>, 2003.
- [36] C. G. Broyden, "A class of methods for solving nonlinear simultaneous equations," *Math. Comput.*, vol. 19, pp. 577–593, 1965.
- [37] S. Bila, D. Baillargeat, S. Verdeyme, and P. Guillon, "Automated design of microwave devices using full EM optimization method," in *IEEE MTT-S Int. Microwave Symp. Dig.*, Baltimore, MD, 1998, pp. 1771–1774.
- [38] A. M. Pavio, "The electromagnetic optimization of microwave circuits using companion models," presented at the IEEE MTT-S Int. Microwave Symp. Workshop, Anaheim, CA, 1999.
- [39] J. W. Bandler, S. H. Chen, S. Daijavad, and K. Madsen, "Efficient optimization with integrated gradient approximations," *IEEE Trans. Microwave Theory Tech.*, vol. 36, pp. 444–455, Feb. 1988.
- [40] M. H. Bakr, J. W. Bandler, K. Madsen, and J. Søndergaard, "Review of the space mapping approach to engineering optimization and modeling," *Optimization Eng.*, vol. 1, pp. 241–276, 2000.
- [41] G. L. Matthaei, "Interdigital band-pass filters," *IEEE Trans. Microwave Theory Tech.*, vol. MTT-10, pp. 479–491, Nov. 1962.
- [42] R. J. Wenzel, "Exact theory of interdigital band-pass filters and related coupled structures," *IEEE Trans. Microwave Theory Tech.*, vol. MTT-13, pp. 559–575, 1965.
- [43] J. W. Bandler, Q. J. Zhang, and R. M. Biernacki, "A unified theory for frequency-domain simulation and sensitivity analysis of linear and nonlinear circuits," *IEEE Trans. Microwave Theory Tech.*, vol. 36, pp. 1661–1669, Dec. 1988.
- [44] J. W. Bandler, Q. J. Zhang, J. Song, and R. M. Biernacki, "FAST gradient based yield optimization of nonlinear circuits," *IEEE Trans. Microwave Theory Tech.*, vol. 38, pp. 1701–1710, Nov. 1990.
- [45] F. Alessandri, M. Mongiardo, and R. Sorrentino, "New efficient full wave optimization of microwave circuits by the adjoint network method," *IEEE Microwave Guided Wave Lett.*, vol. 3, pp. 414–416, Nov. 1993.

- [46] N. K. Georgieva, S. Glavic, M. H. Bakr, and J. W. Bandler, "Feasible adjoint sensitivity technique for EM design optimization," *IEEE Trans. Microwave Theory Tech.*, vol. 50, pp. 2751–2758, Dec. 2002.
- [47] —, "Adjoint variable method for design sensitivity analysis with the method of moments," in *Applied Computational Electromagnetics Soc. Conf.*, Monterey, CA, 2002, pp. 195–201.
- [48] N. K. Nikolova, J. W. Bandler, and M. H. Bakr, "Adjoint techniques for sensitivity analysis in high-frequency structure CAD," *IEEE Trans. Microwave Theory Tech.*, vol. 52, pp. 403–419, Jan. 2004.
- [49] R. Fletcher, *Practical Methods of Optimization*, 2nd ed. New York: Wiley, 1987.
- [50] J. Hald and K. Madsen, "Combined LP and quasi-Newton methods for nonlinear L_1 optimization," *SIAM J. Numer. Anal.*, vol. 22, pp. 68–80, 1985.
- [51] —, "Combined LP and quasi-Newton methods for minimax optimization," *Math. Programming*, vol. 20, pp. 49–62, 1981.
- [52] K. Madsen, "An algorithm for minimax solution of overdetermined systems of nonlinear equations," *J. Inst. Math. Applicat.*, vol. 16, pp. 321–328, 1975.
- [53] —, "Minimax solution of nonlinear equations without calculating derivatives," *Math. Programming Study*, vol. 3, pp. 110–126, 1975.
- [54] J. E. Dennis, Jr. and R. B. Schnabel, *Numerical Methods for Unconstrained Optimization and Nonlinear Equations*, ser. Comput. Math. Englewood Cliffs, NJ: Prentice-Hall, 1983, ch. 10.
- [55] J. J. Moré and D. C. Sorenson, "Computing a trust region step," *SIAM J. Sci. Stat. Comp.*, vol. 4, pp. 553–572, 1983.
- [56] J. W. Bandler, R. M. Biernacki, S. H. Chen, W. J. Getsinger, P. A. Grobelny, C. Moskowitz, and S. H. Talisa, "Electromagnetic design of high-temperature superconducting microwave filters," *Int. J. Microwave Millimeter-Wave Computer-Aided Eng.*, vol. 5, pp. 331–343, 1995.
- [57] J. W. Bandler, M. A. Ismail, and J. E. Rayas-Sánchez, "Expanded space mapping EM-based design framework exploiting preassigned parameters," *IEEE Trans. Circuits Syst. I*, vol. 49, pp. 1833–1838, Dec. 2002.
- [58] J. W. Bandler, M. A. Ismail, and J. E. Rayas-Sánchez, "Broadband physics-based modeling of microwave passive devices through frequency mapping," *Int. J. RF Microwave Computer-Aided Eng.*, vol. 11, pp. 156–170, 2001.
- [59] J. W. Bandler, R. M. Biernacki, S. H. Chen, and Q. H. Wang, "Multiple space mapping EM optimization of signal integrity in high-speed digital circuits," in *Proc. 5th Int. Integrated Nonlinear Microwave and Millimeter Wave Circuits Workshop*, Duisburg, Germany, 1998, pp. 138–140.
- [60] M. Dydyk, "Master the T-junction and sharpen your MIC designs," *Microwaves*, pp. 184–186, 1977.
- [61] J. W. Bandler, M. H. Bakr, N. Georgieva, M. A. Ismail, and D. G. Swanson, Jr., "Recent results in electromagnetic optimization of microwave components including microstrip T-junctions," in *Applied Computational Electromagnetics Soc. Conf.*, Monterey, CA, 1999, pp. 326–333.
- [62] P. M. Watson and K. C. Gupta, "Design and optimization of CPW circuits using EM-ANN models for CPW components," *IEEE Trans. Microwave Theory Tech.*, vol. 45, pp. 2515–2523, Dec. 1997.
- [63] —, "EM-ANN models for microstrip vias and interconnects in multilayer circuits," *IEEE Trans. Microwave Theory Tech.*, vol. 44, pp. 2495–2503, Dec. 1996.
- [64] P. M. Watson, K. C. Gupta, and R. L. Mahajan, "Development of knowledge based artificial neural networks models for microwave components," in *IEEE MTT-S Int. Microwave Symp. Dig.*, Baltimore, MD, 1998, pp. 9–12.
- [65] F. Wang and Q. J. Zhang, "Knowledge based neuromodels for microwave design," *IEEE Trans. Microwave Theory Tech.*, vol. 45, pp. 2333–2343, Dec. 1997.
- [66] F. Wang, "Knowledge based neural networks for microwave modeling and design," Ph.D. dissertation, Dept. Electron., Carleton Univ., Ottawa, ON, Canada, 1998.
- [67] P. M. Watson, G. L. Creech, and K. C. Gupta, "Knowledge based EM-ANN models for the design of wide bandwidth CPW patch/slot antennas," in *IEEE AP-S Int. Symp. Dig.*, Orlando, FL, 1999, pp. 2588–2591.
- [68] J. E. Rayas-Sánchez, "EM-based optimization of microwave circuits using artificial neural networks: The state-of-the-art," *IEEE Trans. Microwave Theory Tech.*, vol. 52, pp. 420–435, Jan. 2004.
- [69] J. W. Bandler, S. H. Chen, R. M. Biernacki, L. Gao, K. Madsen, and H. Yu, "Huber optimization of circuits: A robust approach," *IEEE Trans. Microwave Theory Tech.*, vol. 41, pp. 2279–2287, Dec. 1993.
- [70] J. W. Bandler, J. E. Rayas-Sánchez, and Q. J. Zhang, "Yield-driven electromagnetic optimization via space mapping-based neuromodels," *Int. J. RF Microwave Computer-Aided Eng.*, vol. 12, pp. 79–89, 2002.
- [71] S. J. Leary, A. Bhaskar, and A. J. Keane, "A constraint mapping approach to the structural optimization of an expensive model using surrogates," *Optimization Eng.*, vol. 2, pp. 385–398, 2001.
- [72] M. Redhe, "Simulation based design-structural optimization at early design stages," Masters thesis 922, Dept. Mech. Eng., Div. Solid Mech., Linköping Univ., Linköping, Sweden, 2001.
- [73] M. Redhe and L. Nilsson, "Using space mapping and surrogate models to optimize vehicle crashworthiness design," presented at the 9th AIAA/ISSMO Multidisciplinary Analysis and Optimization Symp., Atlanta, GA, 2002, Paper AIAA-2002-5536.
- [74] V. Devabhaktuni, B. Chattaraj, M. C. E. Yagoub, and Q. J. Zhang, "Advanced microwave modeling framework exploiting automatic model generation, neural networks and space mapping," in *IEEE MTT-S Int. Microwave Symp. Dig.*, Seattle, WA, 2002, pp. 1097–1100.
- [75] D. G. Swanson, Jr. and R. J. Wenzel, "Fast analysis and optimization of combline filters using FEM," in *IEEE MTT-S Int. Microwave Symp. Dig.*, Phoenix, AZ, 2001, pp. 1159–1162.
- [76] P. Harscher, E. Ofli, R. Vahldieck, and S. Amari, "EM-simulator based parameter extraction and optimization technique for microwave and millimeter wave filters," in *IEEE MTT-S Int. Microwave Symp. Dig.*, Seattle, WA, 2002, pp. 1113–1116.
- [77] P. Draxler, "CAD of integrated passives on printed circuit boards through utilization of multiple material domains," in *IEEE MTT-S Int. Microwave Symp. Dig.*, Seattle, WA, 2002, pp. 2097–2100.
- [78] S. Ye and R. R. Mansour, "An innovative CAD technique for microstrip filter design," *IEEE Trans. Microwave Theory Tech.*, vol. 45, pp. 780–786, May 1997.
- [79] J. Snel, "Space mapping models for RF components," presented at the IEEE MTT-S Int. Microwave Symp. Workshop, Phoenix, AZ, 2001.
- [80] A. M. Pavio, J. Estes, and L. Zhao, "The optimization of complex multilayer microwave circuits using companion models and space mapping techniques," presented at the IEEE MTT-S Int. Microwave Symp. Workshop, Seattle, WA, 2002.
- [81] J.-W. Lobeek, "Space mapping in the design of cellular PA output matching circuits," presented at the IEEE MTT-S Int. Microwave Symp. Workshop, Seattle, WA, 2002.
- [82] S. Safavi-Naeini, S. K. Chaudhuri, N. Damavandi, and A. Borji, "A multi-level design optimization strategy for complex RF/microwave structures," presented at the IEEE MTT-S Int. Microwave Symp. Workshop, Seattle, WA, 2002.
- [83] D. Pelz, "Coupled resonator filter realization by 3D-EM analysis and space mapping," presented at the IEEE MTT-S Int. Microwave Symp. Workshop, Seattle, WA, 2002.
- [84] K.-L. Wu, M. Ehlert, and C. Barratt, "An explicit knowledge-embedded space mapping scheme for design of LTCC RF passive circuits," presented at the IEEE MTT-S Int. Microwave Symp. Workshop, Seattle, WA, 2002.
- [85] W. Steyn, R. Lehmsiek, and P. Meyer, "Integrated CAD procedure for IRIS design in a multi-mode waveguide environment," in *IEEE MTT-S Int. Microwave Symp. Dig.*, Phoenix, AZ, 2001, pp. 1163–1166.
- [86] P. Soto, A. Bergner, J. L. Gomez, V. E. Boria, and H. Esteban, "Automated design of inductively coupled rectangular waveguide filters using space mapping optimization," presented at the Eur. Congr. on Computational Methods in Applied Science and Engineering, Barcelona, Spain, Sept. 2000.
- [87] J. V. Morro, H. Esteban, P. Soto, V. E. Boria, C. Bachiller, S. Cogollos, and B. Gimeno, "Automated design of waveguide filters using aggressive space mapping with a segmentation strategy and hybrid optimization techniques," in *IEEE MTT-S Int. Microwave Symp. Dig.*, Philadelphia, PA, 2003, pp. 1215–1218.
- [88] H.-S. Choi, D. H. Kim, I. H. Park, and S. Y. Hahn, "A new design technique of magnetic systems using space mapping algorithm," *IEEE Trans. Magn.*, vol. 37, pp. 3627–3630, Sept. 2001.
- [89] M. A. Ismail, D. Smith, A. Albert, Y. Wang, and M. Yu, "EM based design of large-scale dielectric resonator multiplexers by space mapping," in *IEEE MTT-S Int. Microwave Symp. Dig.*, Philadelphia, PA, 2003, pp. 291–294.
- [90] L. Zhang, J. J. Xu, M. C. E. Yagoub, R. T. Ding, and Q. J. Zhang, "Neuro-space mapping technique for nonlinear device modeling and large signal simulation," in *IEEE MTT-S Int. Microwave Symp. Dig.*, Philadelphia, PA, 2003, pp. 173–176.
- [91] J. E. Dennis, Jr., "A summary of the Danish Technical University November 2000 Workshop," Dept. Comput. Appl. Math., Rice Univ., Houston, TX, Nov. 2000.

- [92] J. W. Bandler and K. Madsen, "Editorial—Surrogate modelling and space mapping for engineering optimization," *Optimization Eng.*, vol. 2, pp. 367–368, 2001.
- [93] J. E. Dennis, Jr., A summary of the Danish Technical University November 2000 Workshop, Dept. Comput. Appl. Math., Rice Univ., Houston, TX, 2001, 2002, private communication.
- [94] J. W. Bandler, Q. S. Cheng, D. H. Gebre-Mariam, K. Madsen, F. Pedersen, and J. Søndergaard, "EM-based surrogate modeling and design exploiting implicit, frequency and output space mappings," in *IEEE MTT-S Int. Microwave Symp. Dig.*, Philadelphia, PA, 2003, pp. 1003–1006.



John W. Bandler (S'66–M'66–SM'74–F'78) was born in Jerusalem, on November 9, 1941. He studied at Imperial College of Science and Technology, London, U.K., from 1960 to 1966. He received the B.Sc. (Eng.), Ph.D., and D.Sc. (Eng.) degrees from the University of London, London, U.K., in 1963, 1967, and 1976, respectively.

In 1966, he joined Mullard Research Laboratories, Redhill, Surrey, U.K. From 1967 to 1969, he was a Post-Doctorate Fellow and Sessional Lecturer with the University of Manitoba, Winnipeg, MB, Canada.

In 1969, he joined McMaster University, Hamilton, ON, Canada, where he has served as Chairman of the Department of Electrical Engineering and Dean of the Faculty of Engineering. He is currently Professor Emeritus in Electrical and Computer Engineering, and directs research in the Simulation Optimization Systems Research Laboratory. He was President of Optimization Systems Associates Inc. (OSA), which he founded in 1983, until November 20, 1997, the date of acquisition of OSA by the Hewlett-Packard Company (HP). OSA implemented a first-generation yield-driven microwave CAD capability for Raytheon in 1985, followed by further innovations in linear and nonlinear microwave CAD technology for the Raytheon/Texas Instruments Joint Venture MIMIC Program. OSA introduced the computer-aided engineering (CAE) systems RoMPE in 1988, HarPE in 1989, OSA90 and OSA90/hope in 1991, Empipe in 1992, and Empipe3D and EmpipeExpress in 1996. OSA created *empath* in 1996, marketed by Sonnet Software Inc. He is currently President of Bandler Corporation, Dundas, ON, Canada, which he founded in 1997. He has authored or coauthored over 350 papers from 1965 to 2003. He contributed to *Modern Filter Theory and Design* (New York: Wiley-Interscience, 1973) and *Analog Methods for Computer-aided Analysis and Diagnosis* (New York: Marcel Dekker Inc., 1988). Four of his papers have been reprinted in *Computer-Aided Filter Design* (New York: IEEE Press, 1973), one in each of *Microwave Integrated Circuits* (Norwood, MA: Artech House, 1975), *Low-Noise Microwave Transistors and Amplifiers* (New York: IEEE Press, 1981), *Microwave Integrated Circuits, 2nd ed.* (Norwood, MA: Artech House, 1985), *Statistical Design of Integrated Circuits* (New York: IEEE Press, 1987), and *Analog Fault Diagnosis* (New York: IEEE Press, 1987). He joined the Editorial Boards of the *International Journal of Numerical Modeling* (1987), the *International Journal of Microwave and Millimeterwave Computer-Aided Engineering* (1989), and *Optimization Eng.* in 1998. He was Guest Editor of the *International Journal of Microwave and Millimeter-Wave Computer-Aided Engineering* Special Issue on Optimization-Oriented Microwave CAD (1997). He was Guest Co-Editor of the *Optimization Eng.* Special Issue on Surrogate Modelling and Space Mapping for Engineering Optimization (2001).

Dr. Bandler is a Fellow of the Canadian Academy of Engineering, the Royal Society of Canada, the Institution of Electrical Engineers (U.K.), and the Engineering Institute of Canada. He is a member of the Association of Professional Engineers of the Province of Ontario (Canada) and a member of the Massachusetts Institute of Technology (MIT) Electromagnetics Academy. He was an associate editor of the IEEE TRANSACTIONS ON MICROWAVE THEORY AND TECHNIQUES (1969–1974), and has continued serving as a member of the Editorial Board. He was guest editor of the IEEE TRANSACTIONS ON MICROWAVE THEORY AND TECHNIQUES Special Issue on Computer-Oriented Microwave Practices (1974) and guest co-editor of the IEEE TRANSACTIONS ON MICROWAVE THEORY AND TECHNIQUES Special Issue on Process-Oriented Microwave CAD and Modeling (1992). He was guest editor of the IEEE TRANSACTIONS ON MICROWAVE THEORY AND TECHNIQUES Special Issue on Automated Circuit Design Using Electromagnetic Simulators (1997). He is guest co-editor of the IEEE TRANSACTIONS ON MICROWAVE THEORY AND TECHNIQUES Special Issue on Electromagnetics-Based Optimization of Microwave Components and Circuits (2004). He has served as chair of the MTT-1 Technical Committee on Computer-Aided Design. He was the recipient of the 1994 Automatic Radio Frequency Techniques Group (ARFTG) Automated Measurements Career Award.



Qingsha S. Cheng (S'00) was born in Chongqing, China. He received the B.Eng. and M.Eng. degrees in automation from Chongqing University, Chongqing, China, in 1995 and 1998, respectively, and is currently working toward the Ph.D. degree at McMaster University, Hamilton, ON, Canada.

In September 1998, he joined the Department of Computer Science and Technology, Peking University, Beijing, China. In September 1999, he joined the Simulation Optimization Systems Research Laboratory, Department of Electrical and Computer Engineering, McMaster University. He has served as a Teaching and Research Assistant. His research interests are CAD, modeling of microwave circuits, software design technology and methodologies for microwave CAD.

Mr. Cheng was the recipient of a one-year Nortel Networks Ontario Graduate Scholarship in Science and Technology (OGSST) for the 2001–2002 academic year.



Sameh A. Dakrouy (S'02) was born in Cairo, Egypt, on May 10, 1973. He received the B.Sc. degree (with honors) and M.Sc. degree from Cairo University, Cairo, Egypt, in 1995 and 2001, respectively.

In 1996, he joined the Faculty of Engineering, Cairo University, where he was a Research and Teaching Assistant with the Department of Engineering Mathematics and Physics. In January 2002, he joined the Simulation Optimization Systems Research Laboratory, McMaster University, Hamilton,

ON, Canada. He is currently a Research and Teaching Assistant with the Department of Electrical and Computer Engineering, McMaster University. His doctoral research concerns recent advances in space-mapping optimization and modeling for microwave circuits.



Ahmed S. Mohamed (S'00) was born in Cairo, Egypt, in 1973. He received the B.Sc. degree (with distinction) in electronics and communications engineering and the Master's degree in engineering mathematics from Cairo University, Cairo, Egypt, in 1995 and 2000, respectively, and is currently working toward the Ph.D. degree at McMaster University, Hamilton, ON, Canada. His Master's thesis concerned time series forecasting using mixtures of neural networks and conventional models.

In September 1995, he joined the Faculty of Engineering, Department of Engineering Mathematics and Physics, Cairo University, as a Teaching and Research Assistant. In September 2000, he joined the Department of Electrical and Computer Engineering, McMaster University. His current research is carried out in the Simulation Optimization Systems Research Laboratory. He is interested in EM optimization methods, microwave CAD, neural-network applications, and modeling of microwave circuits.

Mr. Mohamed was the recipient of a one-year Ontario Graduate Scholarship (OGS) for the 2003–2004 academic year.



Mohamed H. Bakr (S'98–M'01) received the B.Sc. degree (with honors) in electronics and communications engineering and Master's degree in engineering mathematics from Cairo University, Cairo, Egypt, in 1992 and 1996, respectively, and the Ph.D. degree in 2000 from the Department of Electrical and Computer Engineering, McMaster University, Hamilton, ON, Canada.

In 1997, he was a student intern with Optimization Systems Associates Inc. (OSA), Dundas, ON, Canada. From 1998 to 2000, he was a Research Assistant with the Simulation Optimization Systems (SOS) Research Laboratory, McMaster University. In November 2000, he joined the Computational Electromagnetics Research Laboratory (CERL), University of Victoria, Victoria, BC, Canada, as a Natural Sciences and Engineering Research Council of Canada (NSERC) Post-Doctoral Fellow. He is currently an Assistant Professor with the Department of Electrical and Computer Engineering, McMaster University. His research interests include optimization methods, CAD and modeling of microwave circuits, neural-network applications, and smart analysis of microwave circuits and efficient optimization using time/frequency-domain methods.



Kaj Madsen was born in Hjørring, Denmark, in 1943. He received the Cand.Scient. degree in mathematics from the University of Aarhus, Aarhus, Denmark, in 1968, and the Dr.Techn. degree from the Technical University of Denmark (DTU), Lyngby, Denmark, in 1986.

From 1968 to 1988, he was a Lecturer in numerical analysis, apart from the 1973–1974 academic year, when he was with AERE Harwell, Didcot, U.K. Most of his career has been spent with the Department for Numerical Analysis, DTU, however from 1981 to 1983, he was with the Computer Science Department, Copenhagen University. During the summer of 1978, he visited McMaster University, Hamilton, ON, Canada. In 1988, he became a Full Professor. In 1993, he joined the Department of Mathematical Modelling, DTU, and from 1995 to 2000, he was Head of that department. In 2000, he took active part in forming the new Department of Informatics and Mathematical Modelling, DTU, which includes computer science and applied mathematics. Since January 2001, he has headed that department. His primary fields of interest in teaching and research are nonlinear optimization including space-mapping techniques and global optimization, and validated computing using interval analysis.

Dr. Madsen arranged several international workshops on linear programming, parallel algorithms, and surrogate optimization during the 1990s.



Jacob Søndergaard was born in Copenhagen, Denmark, in 1975. He received the Cand.Polyt. and Ph.D. degrees from the Technical University of Denmark (DTU), Lyngby, Denmark, in 1999 and 2003, respectively.

His fields of interest are numerical analysis and optimization, with particular focus on nonlinear optimization and approximation methods.